

Spatial Autoregressive Models for Ecological Inference

Jay M. Ver Hoef¹, Erin E. Peterson², Mevin B. Hooten³, Ephraim M. Hanks⁴, and Marie-Josée Fortin⁵

¹National Marine Mammal Laboratory, NOAA-NMFS Alaska Fisheries Science Center
7600 Sand Point Way NE, Seattle, WA 98115
tel: (907) 456-1995 E-mail: jay.verhoef@noaa.gov

² ARC Centre for Excellence in Mathematical and Statistical Frontiers (ACEMS) and
the Institute for Future Environments, Queensland University of Technology

³ U.S. Geological Survey, Colorado Cooperative Fish and Wildlife Research Unit,
Department of Fish, Wildlife, and Conservation Biology
Department of Statistics, Colorado State University

⁴ Department of Statistics, The Pennsylvania State University

⁵ Department of Ecology and Evolutionary Biology, University of Toronto

May 24, 2016

Abstract

We review conditional autoregressive (CAR) and simultaneous autoregressive (SAR) models for spatial ecological data because they are under-used, or used incorrectly, and this is likely because they are more difficult to understand than geostatistical models. To highlight their usefulness, we identify and discuss six different types of ecological inference using CAR and SAR models, including model selection, spatial regression, estimation of autocorrelation, estimation of other connectivity parameters, spatial prediction, and spatial smoothing. We compare and contrast CAR and SAR models, showing their development and connection to partial correlations. Special cases, such as the intrinsic autoregressive model (IAR), are also shown. Practical use of CAR and SAR models depends on weight matrices, and neighborhood definition and row-standardization are important concepts when developing such matrices. Weight matrices can also include ecological covariates and connectivity structures, which we emphasize but have been rarely used. Trends in harbor seals (*Phoca vitulina*) in southeastern Alaska from 463 polygons, some with missing data, are used to illustrate the six inference types and highlight discussion points from the earlier review. We develop a variety of weight matrices and corresponding CAR and SAR models are fit to data using maximum likelihood and Bayesian methods. We compare models and present spatial regression results for several of these models. Profile likelihood graphs illustrate inference for covariance parameters. The same data set is used for both prediction and smoothing, and the relative merits of each are discussed. We show the nonstationary variances and correlations of a CAR model and demonstrate the effect of row-standardization. We highlight several reasons why ecologists will want to make use of autoregressive models, both directly and in hierarchical models, and not only in explicit spatial settings, but also for more general connectivity models (also known graphical models in mathematics). We conclude with some take-home messages for CAR and SAR models, including 1) thoughts on choosing between CAR and IAR models, 2) modeling ecological effects in the covariance matrix, 3) the appeal of spatial smoothing, 4) how to handle isolated neighbors, and 5) software considerations.

KEY WORDS: Conditional autoregressive, simultaneous autoregressive, CAR, SAR, IAR, geostatistics, prediction, smoothing

INTRODUCTION

When data are collected at spatial locations, Cressie (1993, p. 8) divides spatial statistical models into two broad classes: 1) point-referenced geostatistical models, and 2) lattice models, also called areal models (Banerjee et al., 2014). The two most common lattice models are the conditional autoregressive (CAR) and simultaneous autoregressive (SAR) models. The defining characteristic for CAR and SAR models is that the data occur on a (possibly irregular) grid, or lattice, with a countable set of nodes. Geostatistical models, on the other hand, are used for data that are spatially continuous (i.e., a continuous surface). Another distinction that we find more useful for conceptual understanding is that geostatistical models use spatial information to directly model a covariance matrix, whereas CAR and SAR models use spatial information to model the inverse of a covariance matrix (also known as the precision matrix). Modeling the precision matrix is less intuitive than modeling the covariance matrix, which may make it more difficult to understand the implications of modeling decisions. Indeed, in certain circumstances, Wall (2004) found some surprising and unusual behavior for CAR and SAR models. The less intuitive precision matrix, and a reputation for unusual behavior, may unfortunately keep some scientists from using these models, or inference from the model may be used incorrectly. For example, some highly cited ecological papers have incorrectly compared CAR/SAR to geostatistical models, incorrectly formulated the CAR model, and have given incorrect relationships between CAR and SAR models. We do not dwell on these (details are given in Appendix A), but rather they illustrate that good statistical practice with CAR and SAR models depends on more and better information. CAR and SAR models have many useful applications (e.g., Gelfand et al., 2005; Latimer et al., 2006; Magoun et al., 2007; Hanks and Hooten, 2013). Our objective is to review CAR and SAR models in a practical way, so that their potential may be more fully realized and

used by ecologists.

First we motivate the uses of spatial autoregressive models with typical (and not so typical, but useful) objectives for ecological studies (Table 1). For objective 1, model selection, there are a plethora of model comparison methods, or multimodel inferences, based on Akaike Information Criteria (AIC, Akaike, 1973), Bayes Information Criteria (BIC, Schwarz, 1978), etc., that are generally available (see, e.g., Burnham and Anderson, 2002; Hooten and Hobbs, 2015). CAR and SAR covariance matrices may be part of some or all models, and choosing a model, or comparing various CAR and SAR models, may be an important goal of the investigation. In recent theoretical developments, Song and De Oliveira (2012) provided details on comparing various CAR and SAR models by using Bayes factors. Zhu et al. (2010) extended the least absolute shrinkage and selection operator (LASSO, Tibshirani, 1996) using the least angle regression algorithm (LARS, Efron et al., 2004) to CAR and SAR models. For applied examples, Cassemiro et al. (2007) compared classical regression models assuming independence with SAR models while simultaneously selecting covariates using AIC while studying metabolism in amphibians. Qiu and Turner (2015) used SAR models for random errors along with model averaging in a study of landscape heterogeneity. Tognelli and Kelt (2004) compared CAR and SAR based on autocorrelation in residuals, choosing SAR for an analysis of factors affecting mammalian species richness in South America.

For objective 2, regression, an early and influential paper on using CAR models for Scottish lip cancer data (Clayton and Kaldor, 1987) found that the covariate “% agriculture” helped explain lip cancer rates among counties in Scotland, in conjunction with a CAR model for spatial autocorrelation in the errors. For another example, a spatial CAR regression model using wolverine data (Gardner et al., 2010) showed the probability of occupancy depended on covariates related to elevation and human influence in the plots. Returning to an example above, Cassemiro

et al. (2007) found that several environmental predictors, including temperature, net primary productivity, annual actual precipitation, etc., helped explain species richness of amphibians. Agarwal et al. (2005) used a CAR error model to study the effect of landscape variables, including road and population density, on deforestation. Using a SAR model for invasive alien plant species, Dark (2004) found relationships with elevation, road density, and native plant species richness. In many of these models, the autoregressive component was a latent random effect in a generalized linear mixed model, or a hierarchical model, where the response variable was counts (Clayton and Kaldor, 1987), binary (Gardner et al., 2010), or ordinal (Agarwal et al., 2005). Later, we provide more discussion of CAR and SAR in hierarchical models.

Gardner et al. (2010) provided an example for objective 3, autocorrelation, using a Bayesian CAR model to estimate the autocorrelation parameter, along with credible intervals. Lichstein et al. (2002) also provided estimates of the CAR autocorrelation parameter for three different bird species, along with likelihood ratio tests against the null hypothesis that they were zero. Similarly, but for SAR models, Bullock and Burkhart (2005) used likelihood ratio tests to show significant estimates of several thousand tree species/location combinations with both positive and negative autocorrelation parameters.

Objective 4, covariate effects on autocorrelation, is almost never used in ecological models, or in other disciplines. Historically, the neighborhood structure that forms the covariance matrix in CAR and SAR models is considered a nuisance; that is, it is a requirement to acknowledge spatial autocorrelation to make valid inferences on the other objectives in this list. However, in principle, we can consider distance or neighborhood structure as a covariate, and so logically we can extend this to any measurement between pairs of variables (locations). The influence of covariates on autocorrelation is often of interest in ecological studies (Hanks and Hooten, 2013) and we provide an example of how graphical models can be used to address the objective later.

106 An example of objective 5, prediction, for CAR models is given in both Magoun et al.
107 (2007) and Gardner et al. (2010), who modeled occupancy of wolverines from aerial surveys (also
108 see Johnson et al., 2013a). There were three types of observations: 1) plots that were surveyed
109 with observed animals, 2) plots that were surveyed with no animals, and 3) unsurveyed plots.
110 Predictions for unsurveyed plots provided probabilities of wolverine occurrence. Despite these
111 examples, and the fact that geostatistics and time series are largely focused on prediction (at
112 unsampled locations) and forecasting (at unsampled times in the future), respectively, few
113 examples exist for this objective in ecology, or other disciplines.

114 Objective 6, smoothing, is the classic idea behind the Scottish lip cancer data (Clayton and
115 Kaldor, 1987). In this example, all counties have observed cancer rates. To conceptualize the
116 smoothing objective, imagine that disease rates in administrative districts are generally low, say
117 less than 10% based on thousands of samples, but spatially patterned with areas of lower and
118 higher rates. However, one administrative district has but a single sample that is positive for the
119 disease. It would be unrealistic to estimate the whole administrative district to have 100% disease
120 rates based on that single sample. The models of Clayton and Kaldor (1987) created rates that
121 smoothed over observed data by using values from nearby locations to provide better estimates.
122 Since that time, entire books have been written on the subject (e.g., Elliot et al., 2000; Pfeiffer
123 et al., 2008; Lawson, 2013b), and spatial smoothing of diseases form the introductions to CAR
124 and SAR models in many textbooks on spatial statistics (Cressie, 1993; Waller and Gotway, 2004;
125 Schabenberger and Gotway, 2005; Banerjee et al., 2014). Ecologists rarely have complete counts
126 or surveys for areal units, and so this objective is used relatively infrequently, although
127 increasingly advanced instruments (e.g., LIDAR, Campbell and Wynne, 2011) are yielding
128 remotely sensed data with complete spatial coverage. In addition, measurement error can make
129 the smoothing objective desirable in this case.

CAR and SAR models are prevalent in the literature, and the six goals listed above show that these models can be used in many applications for ecological data. Our objectives are as follows: 1) to explain how these models are obtained, 2) provide insight and intuition on how they work, 3) to compare CAR and SAR models, and 4) provide practical guidelines for their use. We provide an example for further illustration of the objectives given in Table 1. We then discuss important topics that have received little attention so far. For example, there is little guidance in the literature on handling isolated (unconnected) sites, or how to choose between a CAR model and a special case of the CAR model, the intrinsic autoregressive model (IAR). We provide such guidance, and finish with five take-home messages that deserve more attention.

SPATIAL AUTOREGRESSIVE MODELS

Spatial autocorrelation, or autocovariance, quantitatively represents the degree of statistical dependence among random variables using spatial relationships (Cressie, 1993). It is a common characteristic of ecological data, which are often collected at specific locations in space and at specific times. Analyzing spatially correlated data may require the use of spatial statistical models if the assumption of independent errors is violated, making many conventional statistical methods inappropriate (Cliff and Ord, 1981).

In general terms, a spatial statistical model accounts for the spatial locations of the data (i.e., spatial indexing) in the probabilistic part of the model. A wide variety of methods have been developed, thus it is useful to start with a general representation of a spatial statistical model, $\{Z(\mathbf{s}) : \mathbf{s} \in D\}$ (Cressie, 1993, pg. 8). Here, Z is an observed or unobserved random variable at location \mathbf{s} , which belongs to the spatial domain of interest D . The random variable could represent the presence or absence of a species, percent canopy cover, allele counts, etc., while the domain of interest could be a study area, a management unit, or a biogeographic region, etc. In

this paper, we focus on spatial models where D is a finite set and where distance is not necessarily uniquely defined. For example, political administrative districts (such as counties, boroughs, etc.) have area, any set of them is a finite number; they are spatially well-defined, generally as a polygon in a geographic information system (GIS), but (Euclidean) distance between areal units is not well-defined because that requires two points in a Euclidean coordinate system. For example, the distance could be measured between any two locations with the polygon pair, such as nearest-outline-to-nearest-outline, or centroid-to-centroid. Rather than model spatial autocovariance based on Euclidean distance, as is common in geostatistics, spatial relationships for areal data are based on a graphical model, or a network, where sites are depicted as nodes, and edges denote connections (using terminology from graphical models). Edges can be defined in many ways, but a common approach is to create an edge between adjoining administrative units.

The covariance matrices of geostatistical models, where \mathbf{s} varies continuously within D , could be used directly to model data from a finite set of locations within D if Euclidean distance was an appropriate way to express their correlation. The main problem with geostatistical models is that they are guaranteed to be valid only for Euclidean metrics. Consider the case where binary values are used to express connections; the resulting topology is no longer guaranteed to be a Euclidean space. For example, Ver Hoef et al. (2006) showed how nodes, connected in a branching network (representing stream nodes), create a topology for which covariance matrices from commonly used geostatistical models are inappropriate. In this case, one possibility is to create models that are appropriate for the topology (e.g., Ver Hoef and Peterson, 2010), but stream networks are a special topology, and such models are not general. Alternatively, the topology could be deformed to match Euclidean space, such as is done in multidimensional scaling (Curriero, 2006), but this suffers from sensitivity to the exact configuration of points. That is, adding or dropping a node changes the multidimensional scaling.

There is a class of statistical models, however, that are ready-made for spatial network models – the spatial autoregressive models. As we demonstrate, these models are specified through the inverse of the covariance matrix, so they are somewhat less intuitive. For that reason, we now discuss them and provide a fuller understanding of their properties.

Spatial autoregressive models are, fundamentally, not spatial at all. They are also known as graphical models (e.g., Lauritzen, 1996; Whittaker, 2009) and as Gaussian Markov random fields (e.g., Rue and Held, 2005). However, when spatial information is used to define nodes and edges, they are also known as lattice models (e.g., Cressie, 1993, pg. 8) or areal models (e.g., Banerjee et al., 2014, pg. 69). These models differ from the geostatistical models because D is fixed and finite, rather than continuous (Cressie, 1993, pg. 8). As mentioned previously, an areal unit may not have a single set of spatial coordinates and thus the data are indexed by i in the graphical model, rather than \mathbf{s} . For example, Z_i is the random variable for the i th node, where $i = 1, 2, \dots, N$.

Consider the spatial regression framework,

$$\mathbf{y} = \mathbf{X}\boldsymbol{\beta} + \mathbf{z} + \boldsymbol{\varepsilon}, \quad (1)$$

where the goal is to model a first-order mean structure that includes covariates (i.e., predictor variables, \mathbf{X} , measured at the nodes), as well as a latent spatial random process \mathbf{z} , where $\mathbf{z} \sim \mathcal{N}(\mathbf{0}, \boldsymbol{\Sigma})$, and independent error $\boldsymbol{\varepsilon}$, where $\boldsymbol{\varepsilon} \sim \mathcal{N}(\mathbf{0}, \sigma_{\varepsilon}^2 \mathbf{I})$. Note that \mathbf{z} is not directly measured, and instead must be inferred using a statistical model. The spatial regression framework becomes a spatial autoregressive model when the covariance matrix, $\boldsymbol{\Sigma}$, takes one of two main forms: 1) the SAR model,

$$\boldsymbol{\Sigma} \equiv \sigma_Z^2 ((\mathbf{I} - \mathbf{B})(\mathbf{I} - \mathbf{B}'))^{-1}, \quad (2)$$

197 or, 2) the CAR model,

$$\mathbf{\Sigma} \equiv \sigma_Z^2(\mathbf{I} - \mathbf{C})^{-1}\mathbf{M}. \quad (3)$$

198 Here, spatial dependence between Z_i and Z_j is modeled by $\mathbf{B} = \{b_{ij}\}$ and $\mathbf{C} = \{c_{ij}\}$ for the SAR
 199 and CAR models, respectively, where $b_{ii} = 0$ and $c_{ii} = 0$ and $\mathbf{M} = \{m_{ij}\}$ is a diagonal matrix
 200 ($m_{ij} = 0 \forall i \neq j$), where m_{ii} is proportional to the conditional variance of Z_i given all of its
 201 neighbors. The spatial dependence matrices are often developed as $\mathbf{B} = \rho\mathbf{W}$ and $\mathbf{C} = \rho\mathbf{W}$, where
 202 \mathbf{W} is a weights matrix and ρ controls the strength of dependence.

203 To help understand autoregressive models, consider partial correlation (e.g., Snedecor and
 204 Cochran, 1980, pg. 361), which is the idea of correlation between two variables after
 205 “controlling,” or holding fixed, the values for all others variables. If $\mathbf{\Sigma}^{-1} = \mathbf{\Omega} = \{\omega_{i,j}\}$, then the
 206 partial correlation between random variable Z_i and Z_j is $-\omega_{ij}/\sqrt{\omega_{ii}\omega_{jj}}$ (Lauritzen, 1996, pg.
 207 120), which, for normally distributed data, is equivalent to conditional dependence. Thus, we can
 208 see that the CAR model, in particular, allows the modeler to directly specify partial correlations
 209 (or covariances), rather than correlation directly. That is, we are in control of specifying the
 210 off-diagonal matrix values of \mathbf{W} in $\mathbf{\Sigma}^{-1} = \sigma_Z^2\mathbf{M}^{-1}(\mathbf{I} - \rho\mathbf{W})$, and therefore we are specifying the
 211 partial correlations. The SAR model case is similar, though instead of directly specifying partial
 212 correlations, as is done with $(\mathbf{I} - \mathbf{C})$ in the CAR model, the SAR specification involves modeling a
 213 square root, $(\mathbf{I} - \mathbf{B})$, of the precision matrix, which encodes partial correlations. Contrast this
 214 with geostatistics, where we are in control of specifying $\mathbf{\Sigma}$, and therefore we are specifying the
 215 correlations. In both cases, we generally use a functional parameterization, rather than specify
 216 every matrix entry individually. For CAR and SAR models, the algorithm is often based on
 217 neighbors (e.g., partial correlation exists between neighbors that share a boundary), and for
 218 geostatistics, the algorithm is based on distance (e.g., correlation depends on an exponential

decay with distance). For CAR models, if $c_{ij} = 0$, they are partially uncorrelated; otherwise there is partial dependence. Note that b_{ii} and c_{ii} are always zero. For \mathbf{z} (a SAR or CAR random variable) to have a proper statistical distribution, ρ must lie in a range of values that allows $(\mathbf{I} - \mathbf{B})(\mathbf{I} - \mathbf{B}')$ or $(\mathbf{I} - \mathbf{C})$ to have an inverse; that is, ρ cannot be chosen arbitrarily, and its range depends on the weights in \mathbf{W} .

The statistical similarities among the SAR and CAR models are obvious; they both rely on a latent Gaussian specification, a weights matrix, and a correlation parameter. In that sense, both the SAR and CAR models can be implemented similarly. However, there are key differences between SAR and CAR models that are fundamentally important because they impact inference gained from these models. As such, we describe each model in more detail, and later we provide more practical advice.

SAR Models

One approach for building the SAR model begins with the usual regression formulation described in Eq. 1. Instead of modeling the correlation of \mathbf{z} directly, an explicit autocorrelation structure is imposed,

$$\mathbf{z} = \mathbf{B}\mathbf{z} + \boldsymbol{\nu}, \quad (4)$$

where the spatial dependence matrix, $\mathbf{B} = \rho\mathbf{W}$, is relating \mathbf{z} to itself, and $\boldsymbol{\nu} \sim \mathcal{N}(\mathbf{0}, \sigma_Z^2\mathbf{I})$. These models are generally attributed to Whittle (1954). Solving for \mathbf{z} , note that $(\mathbf{I} - \mathbf{B})^{-1}$ must exist (Cressie, 1993; Waller and Gotway, 2004), and then \mathbf{z} has zero mean and covariance matrix $\sigma_Z^2((\mathbf{I} - \mathbf{B})(\mathbf{I} - \mathbf{B}'))^{-1}$. The spatial dependence in the SAR model comes from the matrix \mathbf{B} that causes the simultaneous autoregression of each random variable on its neighbors. When constructing $\mathbf{B} = \rho\mathbf{W}$, the weights matrix \mathbf{W} does not have to be symmetric because it does not appear directly in the inverse of the covariance matrix (i.e., precision matrix). However, there are

obvious constraints to allow $(\mathbf{I} - \mathbf{B})(\mathbf{I} - \mathbf{B}')$ to be a precision matrix that are best explored through the eigenvectors and eigenvalues of \mathbf{W} . The matrix \mathbf{W} must be nonsingular; that is, it cannot have any zero eigenvalues. Also, if $\lambda_{[1]} < 0$ is the smallest eigenvalue, and $\lambda_{[N]} > 0$ is the largest eigenvalue of \mathbf{W} , then $1/\lambda_{[1]} < \rho < 1/\lambda_{[N]}$.

The model created by Eq. 1 and Eq. 4 has been termed the “error” model version of SAR models. An alternative is to simultaneously autoregress the response variable and the errors, $\mathbf{y} = \rho\mathbf{W}\mathbf{y} + \mathbf{X}\boldsymbol{\beta} + \boldsymbol{\varepsilon}$ (Anselin, 1988), yielding

$$\mathbf{y} = (\mathbf{I} - \rho\mathbf{W})^{-1}\mathbf{X}\boldsymbol{\beta} + (\mathbf{I} - \rho\mathbf{W})^{-1}\boldsymbol{\varepsilon}, \quad (5)$$

which allows the matrix \mathbf{W} to smooth covariates in \mathbf{X} as well as creating autocorrelation in the error for \mathbf{y} (e.g., Hooten et al., 2013). A final version is to simultaneously autoregress both response and a separate random effect $\boldsymbol{\nu}$ (e.g., Kissling and Carl, 2008),

$$\mathbf{y} = \rho\mathbf{W}\mathbf{y} + \mathbf{X}\boldsymbol{\beta} + \mathbf{W}\mathbf{X}\boldsymbol{\nu} + \boldsymbol{\varepsilon}, \quad (6)$$

which has been called the SAR mixed model.

CAR Models

The term “conditional” in the CAR model is used because each element of the random process is specified conditionally on the values of the neighboring nodes. The CAR model is typically specified as

$$Z_i | \mathbf{z}_{-i} \sim N \left(\sum_{\forall c_{ij} \neq 0} c_{ij} z_j, m_{ii} \right), \quad (7)$$

256 where \mathbf{z}_{-i} is the vector of all Z_j where $j \neq i$, $\mathbf{C} = \rho \mathbf{W}$ is the spatial dependence matrix with c_{ij}
 257 as its i, j th element, $c_{ii} = 0$, and \mathbf{M} is zero except for diagonal elements m_{ii} . Note that m_{ii} may
 258 depend on the values in the i th row of \mathbf{C} . In this parameterization, the conditional mean of each
 259 Z_i is weighted by values at neighboring nodes. The variance component, m_{ii} , is also conditional
 260 on the neighboring nodes and is thus nonstationary, varying with node i . In contrast to SAR
 261 models, it is not obvious that Eq. 7 can lead to a full joint distribution for all random variables;
 262 however, this was demonstrated by Besag (1974) using Brook's lemma (Brook, 1964) and the
 263 Hammersley-Clifford theorem (Hammersley and Clifford, 1971; Clifford, 1990). For \mathbf{z} to have a
 264 proper statistical distribution, $(\mathbf{I} - \mathbf{C})^{-1}$ must exist and $\mathbf{\Sigma} = \sigma_n^2(\mathbf{I} - \mathbf{C})^{-1}\mathbf{M}$ must be symmetric,
 265 which requires that

$$\frac{c_{ij}}{m_{ii}} = \frac{c_{ji}}{m_{jj}}, \quad \forall i, j. \quad (8)$$

266 For CAR models, \mathbf{W} and ρ are constrained in exactly the same way as for SAR models; \mathbf{W} must
 267 be non-singular and $1/\lambda_{[1]} < \rho < 1/\lambda_{[N]}$ for $\lambda_{[1]}$ the smallest, and $\lambda_{[N]}$ the largest eigenvalues of
 268 \mathbf{W} .

269 A special case of the CAR model, called the intrinsic autoregressive model (IAR) (Besag
 270 and Kooperberg, 1995), occurs when the weights in Eq. 7 occur as,

$$Z_i \sim \mathcal{N} \left(\sum_{j \in \mathcal{N}_i} z_j / |\mathcal{N}_i|, \tau^2 / |\mathcal{N}_i| \right), \quad (9)$$

271 where \mathcal{N}_i are all of the locations defined as neighbors of the i th location, $|\mathcal{N}_i|$ is the number of
 272 neighbors of the i th location, and τ^2 is a constant variance parameter. In Eq. 9, each random
 273 variable is the average of its neighbors, and the variance is proportional to the inverse of the
 274 number of neighbors. Next, we discuss the creation of weights based on averages of neighboring
 275 values.

Row-standardization

We begin a discussion of the weights matrix, \mathbf{W} , which applies to both SAR and CAR models. Consider the simplest case, where a one in \mathbf{W} indicates a connection between sites i and j and a zero indicates no such connection. For site i , let us suppose that there are $|\mathcal{N}_i|$ neighbors, so there are $|\mathcal{N}_i|$ ones in the i th row of \mathbf{W} . In terms of constructing random variables, this implies that Z_i is the *sum* of its neighbors, and summing increases variance. Generally, if left uncorrected, it will not be possible to obtain a covariance matrix in this case. As an analog, consider the first-order autoregressive (AR1) model from time series, where $Z_{i+1} = \phi Z_i + \nu_i$, and ν_i is an independent random variable. It is well-known that $\phi = 1$ is a random walk, and anything with $|\phi| \geq 1$ will not have a variance because the series “explodes” (e.g., Hamilton, 1994, pg. 53). There is a similar phenomenon for SAR and CAR models. In our simple example, for the construction $\rho \mathbf{W}$, the value $\rho |\mathcal{N}_i|$ effectively acts like ϕ , and both should be less than 1 to yield a proper statistical model. For example, consider the case where all locations are on an evenly-spaced rectangular grid of infinite size where each node is connected to 4 neighbors, called a rook’s neighborhood; one each up, down, left, and right. It is well-known that spatial autoregressive models for this example must have $|\rho| < 1/4$ (Haining, 1990, pg. 82). More generally, $|\rho| < 1/n$ if all sites have exactly n neighbors, $|\mathcal{N}_i| = n, \forall i$, to keep variance under control. This leads to the idea of row-standardization.

If we divide each row in \mathbf{W} by $w_{i,+} \equiv \sum_j w_{ij}$, then, again thinking in terms of constructing random variables, each Z_i is the *average* of its neighbors, which decreases variance. In general then, regardless of the number of neighbors, when using row standardization, it is sufficient for $|\rho| < 1$, which is very convenient. Row standardization simplifies the bounds of ρ and makes optimization easier to implement. Moreover, consider again the case of an evenly-spaced rectangular grid of points, but this time of finite size, again using a rook’s neighborhood. Using

300 row standardization, points in the interior of the rectangle are averaged over 4 neighbors, and
 301 they will have smaller variance than those at the perimeter, averaged over 3 neighbors, and the
 302 highest variance will be locations in the corners, averaged over 2 neighbors. Hence, in general,
 303 variance increases toward the *perimeter*. Without row standardization, even when ρ controls
 304 overall variance, locations in the *middle*, summed over more neighbors, have higher variance than
 305 those at the perimeter. For an error process in Eq. 1, higher variance near the perimeter makes
 306 more sense, and, with a more natural and consistent range of values for ρ , we highly recommend
 307 row-standardization. For the CAR models, if \mathbf{W}_+ is an asymmetric matrix with each row in \mathbf{W}
 308 divided by $w_{i,+}$, then $m_{ii} = \tau^2/w_{i,+}$ (the i th diagonal element of \mathbf{M}) satisfies Eq. 8, and note
 309 that τ^2 will not be identifiable from σ_Z^2 in Eq. 3, so the row-standardized CAR model can be
 310 written equivalently as,

$$\Sigma = \sigma_Z^2(\mathbf{I} - \rho\mathbf{W}_+)^{-1}\mathbf{M}_+ = \sigma_Z^2(\text{diag}(\mathbf{W}\mathbf{1}) - \rho\mathbf{W})^{-1}, \quad (10)$$

311 where $\mathbf{1}$ is a vector of all ones.

312 Using row-standardization, and setting $\rho = 1$ in Eq. 7 leads to Eq. 9. In our AR1 analogy,
 313 this is equivalent to $\phi = 1$. In this case, Σ^{-1} is singular (i.e., does not have an inverse), and Σ
 314 does not exist. While this may seem undesirable, random walks and Brownian motion are
 315 stochastic processes without covariance matrices. Considering how they are constructed, it helps
 316 to think of the variances and covariances being defined on the increments; the differences between
 317 adjacent variables. For these increments, the variances and covariances are well-defined. The IAR
 318 distribution is improper, however it is similarly well-defined on spatial increments or contrasts. To
 319 make the IAR proper, an additional constraint can be included, $\sum_i Z_i = 0$. In essence, this
 320 constraint allows all of the random effects to vary except one, which is subsequently used to

ensure that the values sum to zero as a whole. Geometrically, the sum-to-zero constraint can be thought of as anchoring the process near zero for the purposes of random errors in a model. With such a constraint, the IAR model is appealing as an error process in Eq. 1, forming a flexible surface where there is no autocorrelation parameter ρ to estimate. The IAR model is called a first-order intrinsic Gaussian Markov random field (Rue and Held, 2005, p. 93); higher orders are possible but we do not discuss them here.

More Weighting – Accounting for Functional and Structural Connectivity

So far, we have reviewed standard spatial autoregressive models. Now, we want to consider their more general formulation as graphical, or network models. In general, the autoregressive component is an “error” process, and not often of primary interest (compared to prediction or estimating fixed effects parameters, β). However, for ecological networks, there is a great deal of interest in studying spatial connectivity, or equivalently spatial autocorrelation. We discuss other weighting schemes for autoregressive models that have been very rarely, or never, used, but would provide valid autocorrelation models for studying connectivity in ecology. In particular, although the decomposition is not unique, we introduce weighting schemes for the \mathbf{W} matrix that can separate and clarify structural and functional components in network connectivity. By structural, we mean correlation that is determined by physical proximity, such as geographic neighborhoods, a distance measure, etc. By functional, we mean correlation that is affected by dispersal, landscape characteristics, and other covariates of interest, which we illustrate next.

Consider a spatial network of nodes and edges, with the response variable measured at nodes, putting us in the setting of SAR and CAR models. Let \mathbf{e}_{ij} be a characteristic of an edge. The structural idea can be contained in the neighborhood structure – the binary representation of connectivity contains the idea of neighborhood structure. Then edge weights, w_{ij} , between the i th

344 and j th nodes could combine functional and structural connectivity if they are modeled as,

$$w_{ij} = \begin{cases} f(\mathbf{e}_{ij}, \boldsymbol{\theta}), & j \in \mathcal{N}_i \\ 0, & j \notin \mathcal{N}_i. \end{cases} \quad (11)$$

345 where $\boldsymbol{\theta}$ is a p -vector of parameters. To clarify, consider the case where \mathbf{x}_i is a vector of p habitat
 346 characteristics of the i th node, $\mathbf{e}_{i,j} = (\mathbf{x}_i + \mathbf{x}_j)/2$, and $f(\mathbf{e}_{ij}, \boldsymbol{\theta}) = \exp(\mathbf{e}_{ij}'\boldsymbol{\theta})$ (Hanks and Hooten,
 347 2013). This allows a model of the effect that habitat characteristics at the nodes has on
 348 connectivity. If $\theta_h < 0$, then an increase in the h th habitat characteristic results in a smaller edge
 349 weight and greater resistance to network connectivity. However, if $\theta_h > 0$, then an increase in the
 350 h th habitat characteristic results in a larger edge weight and less resistance to network
 351 connectivity. In this example, the mean of the habitat characteristics found at the two nodes,
 352 $(\mathbf{x}_i + \mathbf{x}_j)/2$, was used, but any other function of the two values could also be used (e.g., difference)
 353 if it makes ecological sense. Alternatively, $f(\mathbf{e}_{ij}, \boldsymbol{\theta})$ could be something that is directly measured
 354 on edges, such as a sum of pixel weights in a shortest path between two nodes from a habitat map.

355 For a matrix representation of Eq. 11, let $\mathbf{F}(\boldsymbol{\theta})$ be a matrix of functional relationships for *all*
 356 edges, let \mathbf{B} be a binary matrix indicating neighborhood structure, and $\mathbf{W} = \mathbf{F}(\boldsymbol{\theta}) \odot \mathbf{B}$, where \odot
 357 is the Hadamard (direct, or element by element) product. Then $\mathbf{F}(\boldsymbol{\theta}) \odot \mathbf{B}$ allows a decomposition
 358 for exploring structural and functional changes in connectivity by manipulating each separately.
 359 Of course, this must respect the restrictions described above for SAR and CAR models, and the
 360 parameters need to be estimated, which we discuss in the section on fitting methods.

361 Comparing CAR to SAR with Practical Guidelines

362 With a better understanding of SAR and CAR models, we now compare them more closely and
 363 make practical recommendations for their use; see also Wall (2004). First, we generally do not

recommend versions of the SAR model given by Eq. 5 and Eq. 6. It is difficult to understand how smoothing/lagging covariates and extra random effects contribute to model performance, nor to our understanding, and these models performed poorly in ecological tests (Dormann et al., 2007; Kissling and Carl, 2008). Henceforth, we only discuss the error model defined by Eq. 4.

It is well-known that any SAR model can be written as a CAR model, and Cressie (1993, pg. 408) demonstrated how a SAR model with four neighbors (rook’s neighbor) results in a CAR model that involves all eight neighbors (queen’s neighbor) plus rook’s move to the second neighbors. Although it does not appear to be as simple to go from a CAR model to a SAR, contrary to published accounts (Cressie, 1993, pg. 408) and (Banerjee et al., 2014, pg. 86), it is possible (but not uniquely, without further conditions, which we demonstrate in Appendix B). In fact, it is evident from Eq. 2 that specifying first-order neighbors in \mathbf{B} will result in non-zero partial correlations between second-order neighbors because of the product $(\mathbf{I} - \mathbf{B})(\mathbf{I} - \mathbf{B})'$. Hence, SAR models have a reputation as being less “local” than the CAR models. In fact, using the same construction $\rho\mathbf{W}$ for both SAR and CAR models, Wall (2004) showed that correlation (in Σ , not partial correlation) increases more rapidly with ρ in SAR models than CAR models.

Regarding restrictions on ρ , Wall (2004) also showed strange behavior for negative values of ρ . In geostatistics, there are very few models that allow negative spatial autocorrelation, and, when they do, it cannot be strong. Thus, we recommend that in most situations ρ be constrained to be positive. The fact that \mathbf{W} in SAR models is not required to be symmetric may seem to be an advantage over CAR models. However, we point out that this is illusory from a modeling standpoint, although it may help conceptually in formulating the models. For an analogy, again consider the AR1 model from time series. The model is specified as $Z_{i+1} = \phi Z_i + \nu_i$, so it seems like there is dependence only on previous times. However, the correlation matrix is symmetric, and $\text{corr}(Z_i, Z_{i+t}) = \text{corr}(Z_i, Z_{i-t}) = \phi^t$. Note also that this shows that specifying partial

388 correlations as zero (or conditional independence), does not mean that marginal correlation is
 389 zero (i.e., $\text{corr}(Z_i, Z_{i+t}) \neq 0$ for all t lags). The same is true for CAR and SAR models. In fact,
 390 the situation is less clear than for the AR1 models, where $\text{corr}(Z_i, Z_{i+t}) = \phi^t$ regardless of i . For
 391 CAR and SAR models, two sites that have the same “distance” from each other will have
 392 different correlation, depending on whether they are near the center of the spatial network, or
 393 near the perimeter; that is, correlation is nonstationary, just like the variance when we described
 394 row-standardization.

395 **CAR and SAR in Hierarchical Models**

396 We now turn our focus to the use of CAR and SAR spatial models within a hierarchical model.
 397 To discuss these models more specifically and concretely, in the example and following discussion,
 398 consider the following hierarchical structure that forms a general framework for all that follows,

$$\begin{aligned}
 \mathbf{y} &\sim [\mathbf{y}|g(\boldsymbol{\mu}), \boldsymbol{\nu}], \\
 \boldsymbol{\mu} &\equiv \mathbf{X}\boldsymbol{\beta} + \mathbf{z} + \boldsymbol{\varepsilon}, \\
 \mathbf{z} &\sim [\mathbf{z}|\boldsymbol{\Sigma}] \equiv \text{N}(\mathbf{0}, \boldsymbol{\Sigma}), \\
 \boldsymbol{\Sigma}^{-1} &\equiv \mathbf{F}(\mathbf{N}, \mathbf{D}, \rho, \boldsymbol{\theta}, \dots), \\
 \boldsymbol{\varepsilon} &\sim [\boldsymbol{\varepsilon}|\sigma^2] \equiv \text{N}(\mathbf{0}, \sigma^2\mathbf{I}),
 \end{aligned}
 \tag{12}$$

399 where $[\cdot]$ denotes a generic statistical distribution (Gelfand and Smith, 1990), with the variable on
 400 the left of the bar and conditional variables or parameters on the right of the bar. Here, let \mathbf{y}
 401 contain random variables for the potentially observable data, which could be further partitioned
 402 into $\mathbf{y} = (\mathbf{y}'_o, \mathbf{y}'_u)'$, where \mathbf{y}_o are observed and \mathbf{y}_u are unobserved. Then $[\mathbf{y}|g(\boldsymbol{\mu}), \boldsymbol{\nu}]$ is typically the
 403 data model, with a distribution such as Normal (continuous ecological data, such as plant
 404 biomass), Poisson (ecological count data, such as animal abundance), or Bernoulli (ecological

405 binary data, such as occupancy), which depends on a mean $\boldsymbol{\mu}$ with link function g , and other
 406 parameters $\boldsymbol{\nu}$. The mean $\boldsymbol{\mu}$ has the typical spatial-linear mixed-model form, with design matrix \mathbf{X}
 407 (containing covariates, or explanatory variables), regression parameters $\boldsymbol{\beta}$, spatially
 408 autocorrelated errors \mathbf{z} , and independent errors $\boldsymbol{\varepsilon}$. We let the random effects, \mathbf{z} , be a zero-mean
 409 multivariate-normal distribution with covariance matrix $\boldsymbol{\Sigma}$. In a geostatistical spatial-linear
 410 model, we would model $\boldsymbol{\Sigma}$ directly with covariance functions based on distance like the
 411 exponential, spherical, and Matern (Chiles and Delfiner, 1999). The variance σ^2 , of the
 412 independent component $\text{var}(\boldsymbol{\varepsilon}) = \sigma^2 \mathbf{I}$, is called the nugget effect. However, in CAR and SAR
 413 models, and as described above, we model the inverse of the covariance matrix, $\boldsymbol{\Sigma}^{-1}$, also called
 414 the precision matrix. We denote this as a matrix function, \mathbf{F} , that depends on other information
 415 (e.g., a neighborhood matrix $\mathbf{N} = \mathbf{B}$ or \mathbf{C} , a distance matrix \mathbf{D} , and perhaps others). We isolate
 416 the parameter ρ that controls the strength of autocorrelation, and there could be other
 417 parameters contained in $\boldsymbol{\theta}$, that form the functional relationships among $\mathbf{N}, \mathbf{D}, \dots$, and $\boldsymbol{\Sigma}^{-1}$. In a
 418 Bayesian analysis, we could add further priors, but here we provide just the essential model
 419 components that provide most inferences for ecological data. The model component to be
 420 estimated or predicted from Eq. 12 is identified in Table 1. Note that a joint distribution for all
 421 random quantities can be written as $[\mathbf{y}|g(\boldsymbol{\mu}), \boldsymbol{\nu}][\mathbf{z}|\boldsymbol{\Sigma}][\boldsymbol{\varepsilon}|\sigma^2]$, but the only observable data are \mathbf{y} .
 422 The term likelihood is used when the joint distribution is considered a function of all unknowns,
 423 given the observed data, which we denote $L(\cdot|\mathbf{y})$, and this often forms the basis for fitting models
 424 (discussed next) and model comparison (Table 1).

425 **Fitting Methods for Autoregressive Models**

426 Maximum likelihood estimation is one of the most popular estimation methods (Cressie, 1993).
 427 Earlier, when computers were less powerful, methods were devised to trade efficiency (on things

like bias and consistency) for speed, such as pseudolikelihood (Besag, 1975) and coding (Besag, 1974) for CAR models, among others (Cressie, 1993). Both CAR and SAR models are well-suited for maximum likelihood estimation (Banerjee et al., 2014). For spatial models, the main computational burden in geostatistical models is inversion of the covariance matrix; for CAR and SAR models, the inverse of the covariance matrix is what we actually model. Thus, only the determinant of the covariance matrix needs computing, and fast methods are available (Pace and Barry, 1997a,b), while if matrices do need inverting, sparse matrix methods can be used (Rue and Held, 2005). In addition, for Bayesian Markov chain Monte Carlo methods (MCMC; Gelfand and Smith, 1990), CAR models are ready-made for conditional sampling because of their conditional specification.

Spatial autoregressive models are often used in generalized linear models, which can be viewed as hierarchical models, where the spatial CAR model is generally latent in the mean function in a hierarchical modeling framework. Indeed, one of their most popular uses is for “disease-mapping,” whose name goes back to Clayton and Kaldor (1987); see Lawson (2013a) for book-length treatment. These models can be treated as hierarchical models (Cressie et al., 2009), where the data are assumed to be a count model, such as Poisson, but then the log of the mean parameter has a CAR/SAR model to allow for extra-Poisson variation that is spatially patterned (e.g., Ver Hoef and Jansen, 2007). A similar hierarchical framework has been developed as a generalized linear model for occupancy, which is a binary model, but then the logit (or probit) of the mean parameter has a CAR/SAR model to allow for extra-binomial variation that is spatially patterned (Magoun et al., 2007; Gardner et al., 2010; Johnson et al., 2013a; Broms et al., 2014; Poley et al., 2014). CAR and SAR models can be embedded in more complicated hierarchical models as well (e.g., Ver Hoef et al., 2014). Sometimes that may be too slow, and a fast general-purpose approach to fitting these types of hierarchical models, which depends in part on

the sparsity of the CAR covariance matrix, is integrated nested Laplace approximation (INLA, Rue et al., 2009). INLA has been used in generalized linear models for ecological data (e.g., Haas et al., 2011; Aarts et al., 2013), spatial point patterns (Illian et al., 2013), and animal movement models (Johnson et al., 2013b), among others. The growing popularity of INLA is due in part to its fast computing for approximate Bayesian inference on the marginal distributions of latent variables.

EXAMPLE

We used trends in harbor seals (*Phoca vitulina*) to illustrate the models and approaches for inference described in previous sections. The study area is shown in Fig. 1 and contains 463 polygons used as survey sample units along the mainland, and around islands, in Southeast Alaska. Based on genetic sampling, this area has been divided into 5 different “stocks” (or genetic populations). Over a 14-year period, at various intervals per polygon, seals were counted from aircraft. Using those counts, a trend for each polygon was estimated using Poisson regression. Any polygons with less than two surveys were eliminated, along with trends (linear on the log scale) that had estimated variances greater than 0.1. This eliminated sites with small sample sizes. We treated the estimated trends, on the log scale, as raw data, and ignored the estimated variances. These data were chosen to be illustrative because we expected the trends to show geographic patterns (more so than abundance which varied widely in polygons) and stock structure connectivity, along with stock structure differences in mean values. The data were also continuous in value, thus we modeled the trends with normal distributions to keep the modeling simpler and the results more evident. A map of the estimated trend values (that we henceforth treat as raw data) is given in Fig. 2, showing 463 polygons, of which 306 had observed values and 157 were missing.

For neighborhood structures, we considered three levels of neighbors. The first-order neighbors were based on any two polygons sharing one or more boundary point, and were computed using the *poly2nb* function in the *spdep* package (Bivand and Piras, 2015) in R (R Core Team, 2016). Some polygons were isolated, so they were manually connected to the nearest polygon in space using straight-line (Euclidean) distance between polygon centroids. The first-order neighbors are shown graphically in Fig. 3a with a close-up of part of the study area given in Fig. 3b. Let \mathbf{N}_1 be a matrix of binary values, where a 1 indicates two sites are first-order neighbors, and a 0 otherwise. Then second-order neighbors, which include neighbors of first-order neighbors, were easily obtained in the matrix $\mathbf{N}_2 = \mathcal{I}(\mathbf{N}_1^2)$. Here, $\mathcal{I}(\cdot)$ is an indicator function on each element of the matrix, being 0 only when that element is 0, and 1 otherwise. A close-up of some of the second-order neighbors is shown in Fig. 3c. The fourth-order neighbor matrix was obtained as $\mathbf{N}_4 = \mathcal{I}(\mathbf{N}_2^2)$, and a close-up is shown in Fig. 3d.

We considered covariance constructions that elaborated the three different neighborhood definitions. Let $\mathbf{N}_i; i = 1, 2, 4$ be a neighborhood matrix as described in the previous paragraph. Let \mathbf{S} be a matrix of binary values that indicate whether two sites are in different stocks; that is, if site i and j are in the same stock, then $\mathbf{S}[i, j] = 0$, otherwise $\mathbf{S}[i, j] = 1$. Finally, let the i, j th entries in \mathbf{D} be the Euclidean distance between the centroids of the i th and j th polygons. Then the most elaborate CAR/SAR model we considered was

$$\mathbf{W} = \mathbf{N}_i \odot \mathbf{F}(\boldsymbol{\theta}) = \mathbf{N}_i \odot \exp(-\mathbf{S}/\theta_1) \odot \exp(-\mathbf{D}/\theta_2). \quad (13)$$

We use Eq. 13 in Eq. 2 and Eq. 3, where for SAR models $\mathbf{B} = \rho\mathbf{W}$ or $\mathbf{B} = \rho\mathbf{W}_+$, and for CAR models $\mathbf{C} = \rho\mathbf{W}; \mathbf{M} = \mathbf{I}$ or $\mathbf{C} = \rho\mathbf{W}_+; \mathbf{M} = \mathbf{M}_+$. Note that, when considering the spatial regression model in Eq. 1, $\text{var}(\mathbf{y}) = \boldsymbol{\Sigma} + \sigma_\varepsilon^2\mathbf{I}$ would also be possible; for example, for a first-order

CAR model, $\text{var}(\mathbf{y}) = \sigma_Z^2(\mathbf{I} - \rho\mathbf{W})^{-1} + \sigma_\varepsilon^2\mathbf{I}$. However, when $\rho = 0$, then σ_Z^2 and σ_ε^2 are not identifiable. In fact, as ρ goes from 1 to 0, it allows for diagonal elements to dominate in $(\mathbf{I} - \rho\mathbf{W})^{-1}$, and there seems little reason to add $\sigma_\varepsilon^2\mathbf{I}$. We evaluated some models with the additional component $\sigma_\varepsilon^2\mathbf{I}$, but σ_ε^2 was always estimated to be near 0, so few of those models are presented. The exception is the IAR model, where conceptually ρ is fixed at one.

Our construction is unusual due to the $\exp(-\mathbf{S}/\theta_1)$ component. We interpret θ_1 as an among-stock connectivity parameter. Connectivity is of great interest to ecologists, and by its very definition it is about relationships *between* two nodes. Therefore, it is naturally modeled through the covariance matrix, which is also concerned with this *second-order* model property. Recall that, within stock, all entries in \mathbf{S} will be zero, and hence those same entries in $\exp(-\mathbf{S}/\theta_1)$ will be one. Now, if *among* stocks there is little correlation, then θ_1 should be very small, causing those entries in $\exp(-\mathbf{S}/\theta_1)$ to be near zero. On the other hand, if θ_1 is very large, then there will be high correlation among stocks, and thus the stocks are highly connected with respect to the behavior of the response variable, justifying our interpretation of the parameter. When used in conjunction with the neighborhood matrix, the $\exp(-\mathbf{S}/\theta_1)$ component helps determine if there is additional correlation due to stock structure (low values of θ_1) or whether the neighborhood definitions are enough (θ_1 very large).

We fit model Eq. 1 with a variety of fixed effects and covariance structures, and a list of those models is given in Table 2. We fit models using maximum likelihood (except for the IAR model, which does not have a likelihood, as discussed earlier), and details are given in Appendix C. The resulting maximized values of $2 \times \log\text{-likelihood}$ are given in Fig. 4. Of course, some models are generalizations of other models, with more parameters, and will necessarily have a better fit. Methods such as Akaike Information Criteria (AIC, Akaike, 1973), Bayesian Information Criteria (BIC, Schwarz, 1978), or others (see, e.g., Burnham and Anderson, 2002; Hooten and Hobbs,

2015), can be used to select among these models. This is an example of objective 1 listed in Table 1. For AIC, each additional parameter adds a “penalty” of 2 that is subtracted from the maximized $2 \cdot \log$ -likelihood. Fig. 4 shows the number of model parameters along the x-axis, and dashed lines at increments of two help evaluate models. For example, XC4RD has 8 parameters, so it should be at least 2 better than a model with 7 parameters. If one prefers a likelihood-ratio approach, then a model with one more parameter should be better by a χ -squared value on 1 degree of freedom, or 3.841. We note that there appears to be high variability among model fits, depending on the neighborhood structure (Fig. 4). Several authors have decried the general lack of exploration of the effects of neighborhood definition and choice in weights (Best et al., 2001; Earnest et al., 2007), and our results support their contention that this deserves more attention. In particular, it is interesting that row-standardized CAR models give substantially better fits than unstandardized, and CAR is much better than SAR. Also, for row-standardized CAR models, fit worsens going from first-order to second-order neighborhoods, but then improves when going to fourth-order. Also, perhaps not surprising, using distance between centroids had little effect until fourth-order neighborhoods were used. By an AIC criteria, model XC4RD would be the best model. For model XC4RDS, the parameter θ_1 was very large, making $\exp(-\mathbf{S}/\theta_1)$ nearly constant at 1, so this model component could be dropped without changing the likelihood. Also, the addition of the uncorrelated random errors (model XC4RDU) had an estimated variance σ_ϵ^2 near zero, and left the likelihood essentially unchanged.

As an example of objective 2 from Table 1, the estimation of fixed effects parameters, for 3 different models, are given in Table 3. The model is overparameterized, so the parameter μ is essentially the estimate for stock 1. For example, for the XU model, $\exp(-0.079) = 0.92$, giving an estimated trend of about 8% average decrease per year for sites from stock 1. It is significantly different from 0, which is equivalent to no trend, at $\alpha = 0.05$. This inference is obtained by taking

the estimate and dividing by the standard error, and then assuming that ratio is a standard normal distribution under the null hypothesis that $\mu = 0$. The other estimates are *deviations* from μ , so stock 2 is estimated to have $\exp(-0.079 + 0.048) = 0.97$, or a decrease of about 3% per year. A P -value for stock 2 is obtained by assuming that the estimate divided by the standard error has a standard normal distribution under the model of no difference in means, which is 0.111, and is interpreted as the probability of obtaining the stock 2 value, or larger, if it had the same mean as stock 1. It appears that stocks 3–5 have increasing trends, and that they are significantly different from stock 1 at $\alpha = 0.05$. In comparison, model XC4R, using maximum likelihood estimates (MLE), and Bayesian estimates (MCMC), are given in the middle two sets of columns of Table 3. Notice that, for both, the standard errors are larger than for the independence model XU, leading to greater uncertainty about the fixed effects estimates. Also, the Bayesian posterior standard deviations are somewhat larger than those of maximum likelihood. This is often observed in spatial models when using Bayesian methods, where the uncertainty in estimating the covariance parameters is expressed in the standard errors of the fixed effects, whereas for MLE the covariance parameters are fixed at their most likely values. The MLE estimates and standard errors for the best-fitting model, according to AIC (model XC4RD), are shown in the last set of columns in Table 3, which are very similar to the XC4R model. Further contrasts between trends in stocks are possible by using the variance-covariance matrix for the estimated fixed effects for MLE estimates, or finding the posterior distribution of the contrasts using MCMC sampling in a Bayesian approach.

For objective 3 from Table 1, consider the curves in Fig. 5. We fit all combinations of CAR and SAR models, with and without row-standardization, for the first-, second-, and fourth-order neighbors (12 possible models). All such models had 7 parameters, and a few of the models are listed in Table 2. The likelihood profiles for ρ of the three best-fitting models are shown in Fig. 5.

The peak value for XC4R shows that this is the best model, and the MLE for ρ for this model is 0.604. This curve also provides a likelihood-based confidence interval, known as a profile likelihood confidence interval (Box and Cox, 1964), which essentially inverts a likelihood-ratio test. A $100(1 - \alpha)\%$ confidence interval for a given parameter is the set of all values such that a two-sided test of the null hypothesis that the parameter is the maximum likelihood value would not be rejected at the α level of significance (i.e., the MLE value minus a χ -squared value with one degree of freedom, which is 3.841 if $\alpha = 0.05$). These are all values above the dashed line in Fig. 5 for model XC4R, or, in other words, the endpoints of the confidence interval are provided by the intersection of the dashed line with the curve, which has a lower bound of 0.113 and an upper bound of 0.868. We also show the posterior distribution of ρ for the same model, XC4R, using a Bayesian analysis. The posterior mean was 0.687, with a 95% credible interval ranging from 0.315 to 0.933. The Bayesian estimate used improper uniform priors, so the joint posterior distribution of all parameters will be proportional to the likelihood. The difference between the MLE and the Bayesian estimates for the XC4R model is due to the fact that the MLE is the peak of the likelihood jointly (with all other parameters at their peak), whereas the Bayesian posterior is a marginal distribution (all other parameters have essentially been integrated over by the MCMC algorithm). Nonetheless, the MLE and Bayesian inferences are quite similar.

Fig. 6 shows likelihood profiles for the other parameters in the covariance matrix. For the best model, XC4RD, the solid line in Fig. 6a shows a peak for $\log(\theta_2)$ at 3.717, forming the maximum likelihood estimate and relating to objective 4 from Table 1. Once again, we show a dashed line at the maximized $2 \cdot \log$ -likelihood (413.447) minus a χ -squared value at $\alpha = 0.05$ on one degree of freedom (3.841) to help visualize a confidence interval for θ_2 (the profile likelihood confidence interval given by all values of the solid line that are above the dashed line). The log-likelihood drops rapidly from the MLE ($\hat{\theta}_2 = 3.717$) on the left, intersecting the dashed line

and forming a lower bound at 2.894, whereas the upper limit is unbounded. We return to the notion of stock connectivity in Fig. 6b. The profile likelihood for θ_1 for Model XC4RDS is given by the solid line. The likelihood is very flat for larger values of θ_1 , and in fact it is continuously increasing at an imperceptible rate. Thus, the MLE is the largest value in the parameter range, which we clipped at $\log(\theta_1) = 10$. A lower bound is at $\log(\theta_1) = 0.525$, whereas the upper limit is unbounded again.

Continuing with further inferences from the model, we consider prediction (objective 5) from Table 1. Algorithms for both prediction and smoothing are given in Appendix D. Kriging is a spatial prediction method associated with geostatistics (Cressie, 1990). However, for any covariance matrix, the prediction equations can be applied regardless of how that covariance matrix was developed. We used universal kriging, that is, we included stock effects as covariates, (Huijbregts and Matheron, 1971; Cressie, 1993, pg. 151) to predict all unsampled polygons (black polygons in Fig. 2) using the XC4RD model. Note that kriging, as originally formulated, is an exact interpolator (Cressie, 1993, pg. 129) that “honors the data” (Schabenberger and Gotway, 2005, p. 252) by having predictions take on observed values at observed sites. In Fig. 7a we show the raw observations along with the predictions, making a complete map for all sites. Of course, what distinguishes predictions using statistical models, as opposed to deterministic algorithms (e.g., inverse distance weighted, Shepard, 1968) is that statistical predictions provide standard errors for each prediction (Fig. 7B). When kriging is used as an exact interpolator, the values are known at observed sites, so the prediction variances are zero at observed sites. Hence, we only show the prediction standard errors for polygons with missing data.

We also use the more traditional smoother for CAR and SAR models, such as those used in (Clayton and Kaldor, 1987), forming objective 6 from Table 1. For model XC4RD, without any independent component, this is essentially equivalent to leave-one-out-cross-validation. That is,

616 the conditional expectation, which is obtained directly from Eq. 7 (after adjusting for estimated
 617 covariate effects) is used rather than the observed value at each location. When the covariance
 618 matrix is known, for normally distributed data, ordinary kriging is also the conditional
 619 expectation (Cressie, 1993, p. 108, 174). Hence, the predicted and smoothed values, using the
 620 conditional expectation, are given in Fig. 7c; note then, that the predictions are equivalent to
 621 Fig. 7a at the unsampled locations. Two extremes in smoothing approaches are 1) kriging as an
 622 exact predictor, that is, it leaves the data unchanged (Figs. 7a), and 2) removing observed data to
 623 replace them with conditional expectations based on neighbors (Fig. 7c). In fact, both are quite
 624 unusual for a smoothing objective. Generally, a model is adopted with a spatial component, and a
 625 noisy measurement error or independent component. Smoothing then involves finding a
 626 compromise between the spatial component and the raw, observed data. As an example for these
 627 data, consider the XI4RU model, which has an IAR component plus an uncorrelated error
 628 component. The IAR model has very high autocorrelation ($\rho = 1$), but here we allowed it to be a
 629 mixture with uncorrelated error, and the relative values of σ_Z^2 and σ_ε^2 will determine how much
 630 autocorrelation is estimated for the data. Under this model, predictions for observed data can fall
 631 between the very smooth IAR predictions and the very rough observed data. When such a model
 632 is formulated hierarchically (Eq. 12), often in a Bayesian context, predictions will exhibit a
 633 property called shrinkage (Fay and Herriot, 1979), where predictions of observed values are some
 634 compromise between an ultra-smooth fit from a pure IAR model, and the roughness of the raw
 635 data (Fig. 7d). The amount of shrinkage depends on the relative values of σ_Z^2 and σ_ε^2 . In fact, this
 636 is usually the case when CAR and SAR models are used in a generalized linear model setting
 637 because the conditional independence assumption (e.g., of a Poisson distribution) is analogous to
 638 the $\sigma_\varepsilon^2 \mathbf{I}$ component. Note that a Bayesian perspective is not a requirement, a similar objective is
 639 obtained using filtered kriging (Waller and Gotway, 2004, pg. 306) when there are both spatial

and uncorrelated variance components.

Finally, to complete the example, we return to the idea of nonstationarity in variances and covariances. Notice that, as claimed earlier, row-standardization causes variance to decrease with the numbers of neighbors (which are generally greater in the interior of a study area in contrast to the perimeter) for model XC4R (Fig. 8a), but it is not a simple function of neighbors alone, as it depends in complicated ways on the whole graphical (or network) structure. In contrast, variance generally increases with the number of neighbors without row-standardization (model XC4) of the neighborhood matrix (Fig. 8a). Correlation also decreases with neighbor order, although not as dramatically as one might expect (Fig. 8b), and not at all (on average) between first-order to second-order when the neighborhood matrix is not row-standardized. Box plots summarize all possible correlations as a function of distance between centroids (binned into classes, Fig. 8c,d), which show that while correlation generally decreases with distance between centroids, there is a great deal of variation. Also recall that the MLE for ρ for model XC4R was 0.604 (Fig. 5) for the inverse covariance matrix, but for the covariance matrix, correlations are much lower (Fig. 8b-d). Because weights are developed for partial correlations, or for the inverse of the covariance matrix, when we examine the covariance matrix itself, the diagonal elements are non-constant, in contrast to typical geostatistical models. It is important to realize that there is no direct calculation between the estimated ρ value in the CAR or SAR model and the correlations in the covariance matrix; only that higher ρ generally means higher correlations throughout the covariance matrix. One can always invert the fitted CAR or SAR model to obtain the full covariance matrix, and this can then be inspected and summarized if needed (e.g., Fig. 8), and we highly recommend it for model diagnostics and a better understanding of the fitted model.

DISCUSSION AND CONCLUSIONS

We have presented six objectives used for spatial autoregressive models, some of which are common, and others less so. We argued that the development of the weights in modeling the covariance matrix for CAR and SAR models is less intuitive than choosing a covariance model in geostatistics, but intuition can be gained by considering the relationship to partial correlations. We also argued that row standardization is generally a good idea after choosing initial neighborhoods and weights. CAR models will generally be more “local” for a given set of neighbors because, for that same set of neighbors, the SAR model squares the weights matrix, creating neighbors of neighbors in the inverse covariance matrix. The IAR model is a special case of the CAR model that uses row standardization and fixes the autocorrelation parameter at one, which leads to an improper covariance matrix; however, much like a similar AR1 model, or Brownian motion, these are still useful models. We used an example data set by fitting a variety of CAR/SAR models using MLE and MCMC methods to illustrate all six objectives outlined in the Introduction. Here, we provide further discussion on 5 additional take-home messages: 1) thoughts on choosing between CAR and IAR models, 2) modeling ecological effects in the covariance matrix, 3) the appeal of spatial smoothing, 4) how to handle isolated neighbors, and 5) software considerations.

The choice of IAR versus CAR is confusing, and while both are often described in the literature together, there is little guidance on choosing between them. One advantage of the IAR is that it has one less parameter to estimate. It was proposed by Besag and Kooperberg (1995) in part based on the following: they noticed that for a certain CAR model, ρ in Eq. 3 needed to be 0.999972 to have a marginal correlation near 0.75 (indeed, compare the estimate of $\hat{\rho} = 0.604$ in our example yielding the correlations seen in Fig. 8). In many practical applications, ρ was often

685 estimated to be very near 1, so Besag and Kooperberg (1995) suggested the IAR model as a
 686 flexible spatial surface that has one less parameter to estimate. On the other hand, critics
 687 complained that it may force spatial smoothness where none exists (e.g., Leroux et al., 2000). Our
 688 point of view is best explored through the hierarchical model Eq. 12. Consider an example of
 689 count data, where the data model, $\mathbf{y} \sim [\mathbf{y}|g(\boldsymbol{\mu})]$, conditional on the mean $g(\boldsymbol{\mu})$, is composed of
 690 independent Poisson distributions. Hence, there are no extra variance parameters $\boldsymbol{\nu}$, but rather
 691 the independent, nonstationary variance component is already determined because it is equal to
 692 the mean. In this case, we recommend the CAR model to allow flexibility in modeling the
 693 diagonal of the covariance matrix (the CAR model can allow for smaller ρ values, which
 694 essentially allows for further uncorrelated error). On the other hand, if $[\mathbf{y}|g(\boldsymbol{\mu}), \boldsymbol{\nu}]$ has a free
 695 variance parameter in $\boldsymbol{\nu}$ (e.g., the product of independent normal or negative binomial
 696 distributions), then we recommend the IAR model to decrease confounding between the diagonal
 697 of $\boldsymbol{\Sigma}$, essentially controlled by ρ , and the free variance parameter in $\boldsymbol{\nu}$.

698 The results for Figs. 5 and 6 have confidence intervals that are quite wide. In general,
 699 uncertainty is much higher when trying to estimate covariance parameters than regression (fixed
 700 effect) parameters. Nevertheless, the covariance models that we constructed demonstrate that it
 701 is possible to examine the effect of covariates in the covariance structure (see also Hanks and
 702 Hooten, 2013). In other words, it is possible to make inference on connectivity parameters in the
 703 covariance matrix, but, secondly, they may be difficult to estimate with much precision if the data
 704 are measured only on the nodes. In our harbor seal example, when stock effects were put into the
 705 mean structure, there was abundant evidence of different effects, but when that effect was put
 706 into the covariance matrix, the precision was quite low. It is important to put connectivity effects
 707 into the covariance matrix (in many cases, that will be the only place that makes sense), but
 708 realize that they may be difficult to estimate well without large data sets.

From an ecological viewpoint, why do spatial smoothing? In geology, and mining in particular, modelers were often adamant that no smoothing occur (honoring the data). If we assume that the observed values, without error, are part of the process of interest, then notice from Fig. 2 that the largest value is 0.835 from the legend on the right. Recalling that these are trends, on the log scale, the observed value from the data was $\exp(0.835) = 2.3$, or more than doubling each year. That is clearly not a sustainable growth rate and is likely due to small sample sizes and random variation. That same value from Fig. 7c is $\exp(0.039) = 1.04$, or about 4% growth per year, which is a much more reasonable estimate of growth. The largest smoothed value in Fig. 7c, back on the exponential scale, was 1.083, or about 8% growth per year, and the largest value in Fig. 7d, back on the exponential scale, was 1.146, or about 15% growth per year. These values are similar to published estimates of harbor seal growth rates in natural populations (e.g., Hastings et al., 2012). Fig. 7c,d also clarifies the regional trends, which are difficult to see among the noise in Fig. 2 or by simply filling in the missing sites with predictions (Fig. 7a). For these reasons, smoothing is very popular in disease-mapping applications, but it should be equally attractive for a wide variety of ecological applications. In particular, the XI4RU model (Fig. 7d) is appealing because it uses the data to determine the amount of smoothing. However, we also note that when used in hierarchical models where, for the data model, the variance is fixed in relation to the mean (e.g., binomial, Bernoulli, and Poisson), the amount of smoothing will be dictated by the assumed variance of the data model. In such cases, we reiterate the discussion on choosing between CAR and IAR.

A rarely discussed consideration is the case of isolated sites (those with no neighbors) when constructing the neighborhood matrix. Having a row of zeros in \mathbf{B} in Eq. 2, or in \mathbf{C} in Eq. 3, will cause problems. It is even easier to see that we cannot divide by zero in Eq. 9, or during

732 row-standardization. Instead, we suggest that the covariance matrix be constructed as

$$\begin{pmatrix} \sigma_I^2 \mathbf{I} & \mathbf{0} \\ \mathbf{0} & \mathbf{\Sigma} \end{pmatrix},$$

733 where we show the data ordered such that all isolated sites are first, and their corresponding
734 covariance matrix is $\sigma_I^2 \mathbf{I}$. The matrix $\mathbf{\Sigma}$ is the CAR or SAR covariance matrix for the sites
735 connected by neighbors. Note that one of the main issues here is the separation of the variance
736 parameters, σ_I^2 and σ_Z^2 in Eq. 2 or Eq. 3. As seen in Eq. 9, the autoregressive variance is often
737 scaled by the number of neighbors, and because the isolated sites have no neighbors, it is prudent
738 to give them their own variance parameter.

739 Our final take-home message concerns software. Does the software check the weights to
740 ensure the covariance matrix will be proper? It may be computationally expensive to check it
741 internally, which lessens the appeal of the autoregressive models, and the software may trust the
742 user to give it a valid weights matrix. Does the software use row-standardization internally? How
743 does the software handle isolated sites? These are special issues that only pertain to CAR and
744 SAR models, so we suggest investigation of these issues so that the software output can be better
745 understood.

746 In closing, we note that “networks,” and network models, are increasing throughout science,
747 including ecology (Borrett et al., 2014). Looking again at Fig. 3, if we remove the polygon
748 boundaries, these are network models. Spatial information, in the way of neighborhoods, was
749 used to create the networks. Thus, more general concepts for CAR and SAR models are the
750 graphical models (Lauritzen, 1996; Whittaker, 2009). A better understanding of these models will
751 lead to their application as network models when data are collected on the nodes of the network,
752 and they can be extended beyond spatial data. This provides a rich area for further model

development and research that can include, modify, and enhance the autoregressive models.

Acknowledgments

This research began from a working group on network models at the Statistics and Applied Mathematical Sciences (SAMSI) 2014-15 Program on Mathematical and Statistical Ecology. The project received financial support from the National Marine Fisheries Service, NOAA. Aerial surveys were authorized under a Marine Mammal Protection Act General Authorization (LOC No. 14590) issued to the Marine Mammal Laboratory. The findings and conclusions in the paper are those of the author(s) and do not necessarily represent the views of the reviewers nor the National Marine Fisheries Service, NOAA. Any use of trade, product, or firm names does not imply an endorsement by the U.S. Government.

Data and Code Accessibility

An R package called spAREco was created that contains all data and code. This document was created using knitr, and the manuscript combining latex and R code is also included in the package. The package can be downloaded at <https://github.com/jayverhoef/spAREco.git>, with instructions for installing the package.

References

- Aarts, G., Fieberg, J., Brasseur, S., and Matthiopoulos, J. (2013), “Quantifying the effect of habitat availability on species distributions,” *Journal of Animal Ecology*, 82, 1135–1145.
- Agarwal, D. K., Silander, J. A., Gelfand, A. E., Dewar, R. E., and Mickelson, J. G. (2005),

- “Tropical deforestation in Madagascar: analysis using hierarchical, spatially explicit, Bayesian regression models,” *Ecological Modelling*, 185, 105–131.
- Akaike, H. (1973), “Information theory and an extension of the maximum likelihood principle,” in *Second International Symposium on Information Theory*, eds. Petrov, B. and Csaki, F., Budapest: Akademiai Kiado, pp. 267–281.
- Anselin, L. (1988), *Spatial Econometrics: Methods and Models*, Dordrecht, the Netherlands: Kluwer Academic Publishers.
- Banerjee, S., Carlin, B. P., and Gelfand, A. E. (2014), *Hierarchical Modeling and Analysis for Spatial Data*, Boca Raton, FL, USA: Chapman and Hall/CRC Press.
- Beguéría, S. and Pueyo, Y. (2009), “A comparison of simultaneous autoregressive and generalized least squares models for dealing with spatial autocorrelation,” *Global Ecology and Biogeography*, 18, 273–279.
- Besag, J. (1974), “Spatial interaction and the statistical analysis of lattice systems (with discussion),” *Journal of the Royal Statistical Society, Series B*, 36, 192–236.
- (1975), “Statistical analysis of non-lattice data,” *The Statistician*, 179–195.
- Besag, J. and Kooperberg, C. (1995), “On conditional and intrinsic autoregressions,” *Biometrika*, 82, 733–746.
- Best, N., Cockings, S., Bennett, J., Wakefield, J., and Elliott, P. (2001), “Ecological regression analysis of environmental benzene exposure and childhood leukaemia: sensitivity to data inaccuracies, geographical scale and ecological bias,” *Journal of the Royal Statistical Society. Series A (Statistics in Society)*, 164, 155–174.

793 Bivand, R. and Piras, G. (2015), “Comparing implementations of estimation methods for spatial
794 econometrics,” *Journal of Statistical Software*, 63, 1–36.

795 Borrett, S. R., Moody, J., and Edelman, A. (2014), “The rise of network ecology: maps of the
796 topic diversity and scientific collaboration,” *Ecological Modelling*, 293, 111–127.

797 Box, G. E. P. and Cox, D. R. (1964), “An analysis of transformations,” *Journal of the Royal
798 Statistical Society, Series B*, 26, 211–252.

799 Bross, K. M., Johnson, D. S., Altwegg, R., and Conquest, L. L. (2014), “Spatial occupancy
800 models applied to atlas data show Southern Ground Hornbills strongly depend on protected
801 areas,” *Ecological Applications*, 24, 363–374.

802 Brook, D. (1964), “On the distinction between the conditional probability and the joint
803 probability approaches in the specification of nearest-neighbour systems,” *Biometrika*, 481–483.

804 Bullock, B. P. and Burkhart, H. E. (2005), “An evaluation of spatial dependency in juvenile
805 loblolly pine stands using stem diameter,” *Forest Science*, 51, 102–108.

806 Burnham, K. P. and Anderson, D. R. (2002), *Model Selection and Multimodel Inference: A
807 Practical Information-Theoretic Approach*, New York: Springer-Verlag Inc.

808 Campbell, J. B. and Wynne, R. H. (2011), *Introduction to Remote Sensing*, Guilford Press.

809 Cassemiro, F. A., Diniz-Filho, J. A. F., Rangel, T. F. L., and Bini, L. M. (2007), “Spatial
810 autocorrelation, model selection and hypothesis testing in geographical ecology: Implications
811 for testing metabolic theory in New World amphibians,” *Neotropical Biology and Conservation*,
812 2, 119–126.

- 813 Chiles, J.-P. and Delfiner, P. (1999), *Geostatistics: Modeling Spatial Uncertainty*, New York: John
814 Wiley & Sons.
- 815 Clayton, D. and Kaldor, J. (1987), “Empirical Bayes estimates of age-standardized relative risks
816 for use in disease mapping,” *Biometrics*, 43, 671–681.
- 817 Cliff, A. D. and Ord, J. K. (1981), *Spatial Processes: Models and Applications*, vol. 44, London,
818 U.K.: Pion.
- 819 Clifford, P. (1990), “Markov random fields in statistics,” in *Disorder in Physical Systems: A*
820 *Volume in Honour of John M. Hammersley*, eds. Grimmett, R. G. and Welsh, D. J. A., New
821 York, NY, USA: Oxford University Press, pp. 19–32.
- 822 Cressie, N. (1990), “The origins of kriging,” *Mathematical Geology*, 22, 239–252.
- 823 Cressie, N., Calder, K. A., Clark, J. S., Ver Hoef, J. M., and Wikle, C. K. (2009), “Accounting for
824 uncertainty in ecological analysis: The strengths and limitations of hierarchical statistical
825 modeling,” *Ecological Applications*, 19, 553–570.
- 826 Cressie, N. and Wikle, C. K. (2011), *Statistics for Spatio-temporal Data*, Hoboken, New Jersey:
827 John Wiley & Sons.
- 828 Cressie, N. A. C. (1993), *Statistics for Spatial Data, Revised Edition*, New York: John Wiley &
829 Sons.
- 830 Curriero, F. C. (2006), “On the use of non-Euclidean distance measures in geostatistics,”
831 *Mathematical Geology*, 38, 907–926.
- 832 Dark, S. J. (2004), “The biogeography of invasive alien plants in California: an application of GIS
833 and spatial regression analysis,” *Diversity and Distributions*, 10, 1–9.

- Dormann, C. F., McPherson, J. M., Araújo, M. B., Bivand, R., Bolliger, J., Carl, G., Davies,
R. G., Hirzel, A., Jetz, W., Kissling, W. D., Kühn, I., Ohlemüller, R., Peres-Neto, P. R.,
Reineking, B., Schröder, B., Schurr, F. M., and Wilson, R. (2007), “Methods to account for
spatial autocorrelation in the analysis of species distributional data: a review,” *Ecography*, 30,
609–628.
- Earnest, A., Morgan, G., Mengersen, K., Ryan, L., Summerhayes, R., and Beard, J. (2007),
“Evaluating the effect of neighbourhood weight matrices on smoothing properties of
Conditional Autoregressive (CAR) models,” *International Journal of Health Geographics*, 6, 54,
doi = 10.1016/j.csda.2011.10.022.
- Efron, B., Hastie, T., Johnstone, I., and Tibshirani, R. (2004), “Least angle regression,” *The
Annals of Statistics*, 32, 407–499.
- Elliot, P., Wakefield, J. C., Best, N. G., Briggs, D., et al. (2000), *Spatial epidemiology: methods
and applications.*, Oxford, UK: Oxford University Press.
- Fay, R. E. and Herriot, R. A. (1979), “Estimates of income for small places: an application of
James-Stein procedures to census data,” *Journal of the American Statistical Association*, 74,
269–277.
- Gardner, C. L., Lawler, J. P., Ver Hoef, J. M., Magoun, A. J., and Kellie, K. A. (2010),
“Coarse-scale distribution surveys and occurrence probability modeling for wolverine in interior
Alaska,” *The Journal of Wildlife Management*, 74, 1894–1903.
- Gelfand, A. E., Schmidt, A. M., Wu, S., Silander, J. A., Latimer, A., and Rebelo, A. G. (2005),
“Modelling species diversity through species level hierarchical modelling,” *Journal of the Royal
Statistical Society: Series C (Applied Statistics)*, 54, 1–20.

856 Gelfand, A. E. and Smith, A. F. M. (1990), “Sampling-based approaches to calculating marginal
857 densities,” *Journal of the American Statistical Association*, 85, 398–409.

858 Haas, S. E., Hooten, M. B., Rizzo, D. M., and Meentemeyer, R. K. (2011), “Forest species
859 diversity reduces disease risk in a generalist plant pathogen invasion,” *Ecology Letters*, 14,
860 1108–1116.

861 Haining, R. (1990), *Spatial Data Analysis in the Social and Environmental Sciences*, Cambridge,
862 UK: Cambridge University Press.

863 Hamilton, J. D. (1994), *Time Series Analysis*, vol. 2, Princeton, NJ, USA: Princeton University
864 Press.

865 Hammersley, J. M. and Clifford, P. (1971), “Markov fields on finite graphs and lattices,”
866 Unpublished Manuscript.

867 Hanks, E. M. and Hooten, M. B. (2013), “Circuit theory and model-based inference for landscape
868 connectivity,” *Journal of the American Statistical Association*, 108, 22–33.

869 Harville, D. A. (1997), *Matrix Algebra from a Statistician’s Perspective*, New York, NY: Springer.

870 Hastings, K. K., Small, R. J., and Pendleton, G. W. (2012), “Sex-and age-specific survival of
871 harbor seals (*Phoca vitulina*) from Tugidak Island, Alaska,” *Journal of Mammalogy*, 93,
872 1368–1379.

873 Hooten, M. and Hobbs, N. (2015), “A guide to Bayesian model selection for ecologists,” *Ecological*
874 *Monographs*, 85, 3–28.

875 Hooten, M. B., Hanks, E. M., Johnson, D. S., and Alldredge, M. W. (2013), “Reconciling resource
876 utilization and resource selection functions,” *Journal of Animal Ecology*, 82, 1146–1154.

- Huijbregts, C. and Matheron, G. (1971), “Universal kriging (an optimal method for estimating and contouring in trend surface analysis),” in *Proceedings of Ninth International Symposium on Techniques for Decision-making in the Mineral Industry*, ed. McGerrigle, J. I., The Canadian Institute of Mining and Metallurgy, Special Volume 12, pp. 159–169.
- Illian, J. B., Martino, S., Sørbye, S. H., Gallego-Fernández, J. B., Zunzunegui, M., Esquivias, M. P., and Travis, J. M. (2013), “Fitting complex ecological point process models with integrated nested Laplace approximation,” *Methods in Ecology and Evolution*, 4, 305–315.
- Johnson, D. S., Conn, P. B., Hooten, M. B., Ray, J. C., and Pond, B. A. (2013a), “Spatial occupancy models for large data sets,” *Ecology*, 94, 801–808.
- Johnson, D. S., Hooten, M. B., and Kuhn, C. E. (2013b), “Estimating animal resource selection from telemetry data using point process models,” *Journal of Animal Ecology*, 82, 1155–1164.
- Keitt, T. H., Bjørnstad, O. N., Dixon, P. M., and Citron-Pousty, S. (2002), “Accounting for spatial pattern when modeling organism-environment interactions,” *Ecography*, 25, 616–625.
- Kissling, W. D. and Carl, G. (2008), “Spatial autocorrelation and the selection of simultaneous autoregressive models,” *Global Ecology and Biogeography*, 17, 59–71.
- Latimer, A. M., Wu, S., Gelfand, A. E., and Silander Jr, J. A. (2006), “Building statistical models to analyze species distributions,” *Ecological Applications*, 16, 33–50.
- Lauritzen, S. L. (1996), *Graphical Models*, Oxford, UK: Oxford University Press.
- Lawson, A. B. (2013a), *Bayesian Disease Mapping: Hierarchical Modeling in Spatial Epidemiology*, Boca Raton, FL: CRC Press.
- (2013b), *Statistical Methods in Spatial Epidemiology*, Chichester, UK: John Wiley & Sons.

898 Leroux, B. G., Lei, X., and Breslow, N. (2000), “Estimation of disease rates in small areas: A new
 899 mixed model for spatial dependence,” in *Statistical Models in Epidemiology, the Environment,
 900 and Clinical Trials*, eds. Halloran, M. E. and Berry, D. A., Springer, pp. 179–191.

901 Lichstein, J. W., Simons, T. R., Shiner, S. A., and Franzreb, K. E. (2002), “Spatial
 902 autocorrelation and autoregressive models in ecology,” *Ecological Monographs*, 72, 445–463.

903 Lunn, D. J., Thomas, A., Best, N., and Spiegelhalter, D. (2000), “WinBUGS – A Bayesian
 904 modelling framework: concepts, structure, and extensibility,” *Statistics and Computing*, 10,
 905 325–337.

906 Magoun, A. J., Ray, J. C., Johnson, D. S., Valkenburg, P., Dawson, F. N., and Bowman, J.
 907 (2007), “Modeling wolverine occurrence using aerial surveys of tracks in snow,” *Journal of
 908 Wildlife Management*, 71, 2221–2229.

909 Pace, R. K. and Barry, R. (1997a), “Fast spatial estimation,” *Applied Economics Letters*, 4,
 910 337–341.

911 — (1997b), “Sparse spatial autoregressions,” *Statistics & Probability Letters*, 33, 291–297.

912 Pfeiffer, D., Robinson, T., Stevenson, M., Stevens, K. B., Rogers, D. J., and Clements, A. C.
 913 (2008), *Spatial Analysis in Epidemiology*, Oxford, UK: Oxford University Press Oxford.

914 Poley, L. G., Pond, B. A., Schaefer, J. A., Brown, G. S., Ray, J. C., and Johnson, D. S. (2014),
 915 “Occupancy patterns of large mammals in the Far North of Ontario under imperfect detection
 916 and spatial autocorrelation,” *Journal of Biogeography*, 41, 122–132.

917 Qiu, J. and Turner, M. G. (2015), “Importance of landscape heterogeneity in sustaining
 918 hydrologic ecosystem services in an agricultural watershed,” *Ecosphere*, 6, 1–19.

919 R Core Team (2016), *R: A Language and Environment for Statistical Computing*, R Foundation
920 for Statistical Computing, Vienna, Austria.

921 Rue, H. and Held, L. (2005), *Gauss Markov Random Fields: Theory and Applications*, Boca
922 Raton, FL, USA: Chapman and Hall/CRC.

923 Rue, H., Martino, S., and Chopin, N. (2009), “Approximate Bayesian inference for latent
924 Gaussian models by using integrated nested Laplace approximations,” *Journal of the Royal*
925 *Statistical Society: Series B (Statistical Methodology)*, 71, 319–392.

926 Schabenberger, O. and Gotway, C. A. (2005), *Statistical Methods for Spatial Data Analysis*, Boca
927 Raton, Florida: Chapman Hall/CRC.

928 Schwarz, G. (1978), “Estimating the dimension of a model,” *The Annals of Statistics*, 6, 461–464.

929 Shepard, D. (1968), “A two-dimensional interpolation function for irregularly-spaced data,” in
930 *Proceedings of the 1968 23rd ACM National Conference*, ACM, pp. 517–524.

931 Snedecor, G. W. and Cochran, W. G. (1980), *Statistical Methods, Seventh Edition*, Iowa State
932 University.

933 Song, J. J. and De Oliveira, V. (2012), “Bayesian model selection in spatial lattice models,”
934 *Statistical Methodology*, 9, 228–238.

935 Tibshirani, R. (1996), “Regression shrinkage and selection via the lasso,” *Journal of the Royal*
936 *Statistical Society. Series B (Methodological)*, 267–288.

937 Tognelli, M. F. and Kelt, D. A. (2004), “Analysis of determinants of mammalian species richness
938 in South America using spatial autoregressive models,” *Ecography*, 27, 427–436.

- 939 Ver Hoef, J. M., Cameron, M. F., Boveng, P. L., London, J. M., and Moreland, E. E. (2014), “A
940 spatial hierarchical model for abundance of three ice-associated seal species in the eastern
941 Bering Sea,” *Statistical Methodology*, 17, 46–66.
- 942 Ver Hoef, J. M. and Jansen, J. K. (2007), “Space-time zero-inflated count models of Harbor
943 seals,” *Environmetrics*, 18, 697–712.
- 944 Ver Hoef, J. M. and Peterson, E. (2010), “A moving average approach for spatial statistical
945 models of stream networks (with discussion),” *Journal of the American Statistical Association*,
946 105, 6–18.
- 947 Ver Hoef, J. M., Peterson, E. E., and Theobald, D. (2006), “Spatial statistical models that use
948 flow and stream distance,” *Environmental and Ecological Statistics*, 13, 449–464.
- 949 Wall, M. M. (2004), “A close look at the spatial structure implied by the CAR and SAR models,”
950 *Journal of Statistical Planning and Inference*, 121, 311–324.
- 951 Waller, L. A. and Gotway, C. A. (2004), *Applied Spatial Statistics for Public Health Data*, John
952 Wiley and Sons, New Jersey.
- 953 Whittaker, J. (2009), *Graphical Models in Applied Multivariate Statistics*, Chichester, UK: Wiley
954 Publishing.
- 955 Whittle, P. (1954), “On stationary processes in the plane,” *Biometrika*, 41, 434–449.
- 956 Zhu, J., Huang, H.-C., and Reyes, P. E. (2010), “On selection of spatial linear models for lattice
957 data,” *Journal of the Royal Statistical Society: Series B (Statistical Methodology)*, 72, 389–402.

Table 1: Common objectives when using spatial autoregressive models. Notation for the model components comes from Eq. 12.

Objective	Description	Model Component
1. Model Comparison & Selection	CAR and SAR models are often part of a spatial (generalized) linear model. One goal, prior to further inference, might be to compare models, and then choose one. The choice of the form of a CAR or SAR model may be important in this comparison and selection.	$L(\cdot \mathbf{y})$
2. Regression	The goal is to estimate the spatial regression coefficients, which quantify how an explanatory variable “affects” the response variable.	$\boldsymbol{\beta}$
3. Autocorrelation	The goal is to estimate the “strength” of autocorrelation, especially if it represents an ecological idea such as spatial connectivity, which quantifies how similarly sites change in the residual errors, after accounting for regression effects.	ρ
4. Neighborhood Structure	The goal is to estimate covariate effects on neighborhood structure. Although rarely used, covariates can be included in the precision matrix to see how they affect neighborhood structure (causing more or less correlation).	$\boldsymbol{\theta}$
5. Prediction	This is the classical goal of geostatistics, and is rarely used in CAR and SAR models. However, if sites have missing data, prediction is possible.	\mathbf{y}_u and/or $\boldsymbol{\mu}_u$
6. Smoothing	The goal is to create values at spatial sites that smooth over observed data by using values from nearby locations to provide better estimates.	$g(\boldsymbol{\mu})$

Table 2: A variety of candidate models used to explore spatial autoregressive models for the example data set. For fixed effects, the $\mathbf{1}$ indicates an overall mean in the model, and $\mathbf{X}_{\text{stock}}$ includes an additional categorical effect for each stock. A $[\cdot]_+$ around a matrix indicates row-standardization, and for CAR models, $[\mathbf{M}]_+$ is the appropriate diagonal matrix for such row standardization. The matrices themselves are described in the text. For model codes, m indicates an overall mean only, whereas X indicates the additional stock effect in the fixed effects. C indicates a CAR model, S a SAR model, and I an IAR model. A 1 indicates a first-order neighborhood, 2 a second-order neighborhood, and 4 a fourth-order neighborhood. R indicates row-standardization. D indicates inclusion of Euclidean distance within neighborhoods, S a cross stock connectivity matrix. U at the end indicates inclusion of an additive random effect of uncorrelated variables.

Model Code	Fixed Effects	Covariance Model	No. Parms
mU	$\mathbf{1}$	$\sigma_\varepsilon^2 \mathbf{I}$	2
mC1R	$\mathbf{1}$	$\sigma_Z^2 (\mathbf{I} - \rho [\mathbf{W}_1]_+)^{-1} [\mathbf{M}]_+$	3
XU	$\mathbf{X}_{\text{stock}}$	$\sigma_\varepsilon^2 \mathbf{I}$	6
XC1R	$\mathbf{X}_{\text{stock}}$	$\sigma_Z^2 (\mathbf{I} - \rho [\mathbf{W}_1]_+)^{-1} [\mathbf{M}]_+$	7
XC1	$\mathbf{X}_{\text{stock}}$	$\sigma_Z^2 (\mathbf{I} - \rho \mathbf{W}_1)^{-1}$	7
XS1R	$\mathbf{X}_{\text{stock}}$	$\sigma_Z^2 [(\mathbf{I} - \rho [\mathbf{W}_1]_+)(\mathbf{I} - \rho [\mathbf{W}_1]_+)]^{-1}$	7
XS1	$\mathbf{X}_{\text{stock}}$	$\sigma_Z^2 [(\mathbf{I} - \rho \mathbf{W}_1)(\mathbf{I} - \rho \mathbf{W}_1)]^{-1}$	7
XC2R	$\mathbf{X}_{\text{stock}}$	$\sigma_Z^2 (\mathbf{I} - \rho [\mathbf{W}_2]_+)^{-1} [\mathbf{M}]_+$	7
XC4R	$\mathbf{X}_{\text{stock}}$	$\sigma_Z^2 (\mathbf{I} - \rho [\mathbf{W}_4]_+)^{-1} [\mathbf{M}]_+$	7
XC4	$\mathbf{X}_{\text{stock}}$	$\sigma_Z^2 (\mathbf{I} - \rho \mathbf{W}_4)^{-1}$	7
XI4RU	$\mathbf{X}_{\text{stock}}$	$\sigma_Z^2 (\mathbf{I} - [\mathbf{W}_4]_+)^{-1} [\mathbf{M}]_+ + \sigma_\varepsilon^2 \mathbf{I}$ (improper)	7
XC4RD	$\mathbf{X}_{\text{stock}}$	$\sigma_Z^2 (\mathbf{I} - \rho [\mathbf{W}_4 \odot \exp(-\mathbf{D}/\theta_2)]_+)^{-1} [\mathbf{M}]_+$	8
XC4RDS	$\mathbf{X}_{\text{stock}}$	$\sigma_Z^2 (\mathbf{I} - \rho [\mathbf{W}_4 \odot \exp(-\mathbf{D}/\theta_2) \odot \exp(-\mathbf{S}/\theta_2)]_+)^{-1} [\mathbf{M}]_+$	9
XC4RDU	$\mathbf{X}_{\text{stock}}$	$\sigma_Z^2 (\mathbf{I} - \rho [\mathbf{W}_4 \odot \exp(-\mathbf{D}/\theta_2)]_+)^{-1} [\mathbf{M}]_+ + \sigma_\varepsilon^2 \mathbf{I}$	9

Table 3: Estimated fixed effects for several models listed in Table 2. Both the estimate (Est.) and estimated standard error (Std.Err.) are given for each model. All models use maximum likelihood estimates (MLE), except for XC4R model, we distinguish the MLE estimate with -MLE, and a Bayesian estimate using Markov chain Monte Carlo with -MCMC.

Parameter	XU		XC4R-MLE		XC4R-MCMC		XC4RD	
	Est.	Std.Err.	Est.	Std.Err.	Est.	Std.Err.	Est.	Std.Err.
μ	-0.079	0.0225	-0.080	0.0288	-0.082	0.0330	-0.077	0.0290
$\beta_{\text{stock } 2}$	0.048	0.0298	0.063	0.0379	0.063	0.0429	0.058	0.0386
$\beta_{\text{stock } 3}$	0.093	0.0281	0.095	0.0355	0.097	0.0386	0.092	0.0356
$\beta_{\text{stock } 4}$	0.132	0.0279	0.135	0.0346	0.138	0.0406	0.132	0.0346
$\beta_{\text{stock } 5}$	0.084	0.0259	0.093	0.0327	0.096	0.0378	0.089	0.0330

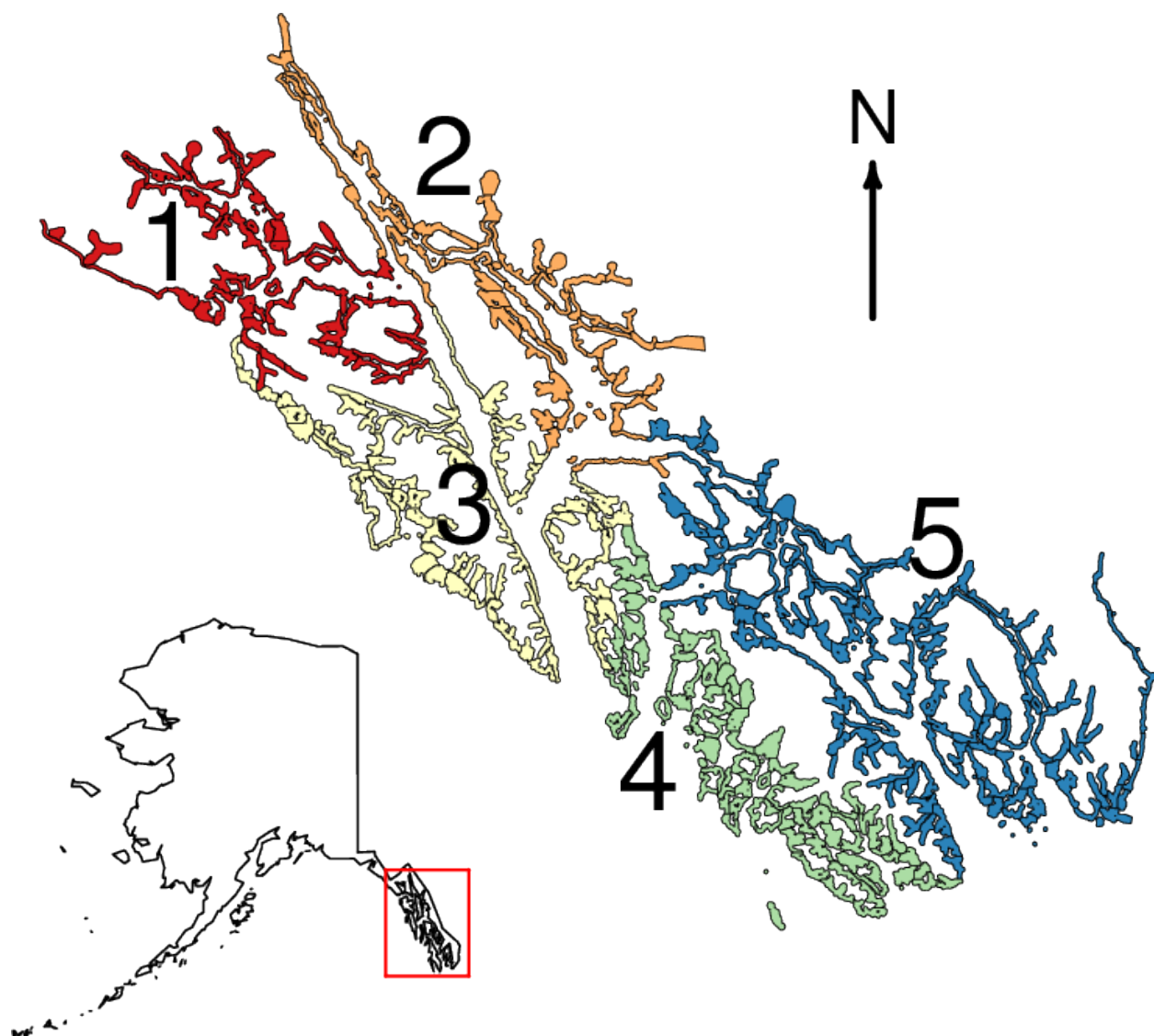


Figure 1: Study area in Southeast Alaska, outlined in red in the lower left figure. Survey polygons were established around the coast of the mainland and all islands, which were surveyed for harbor seals. The study area comprises 5 stocks, each with their own color, and are numbered for further reference.

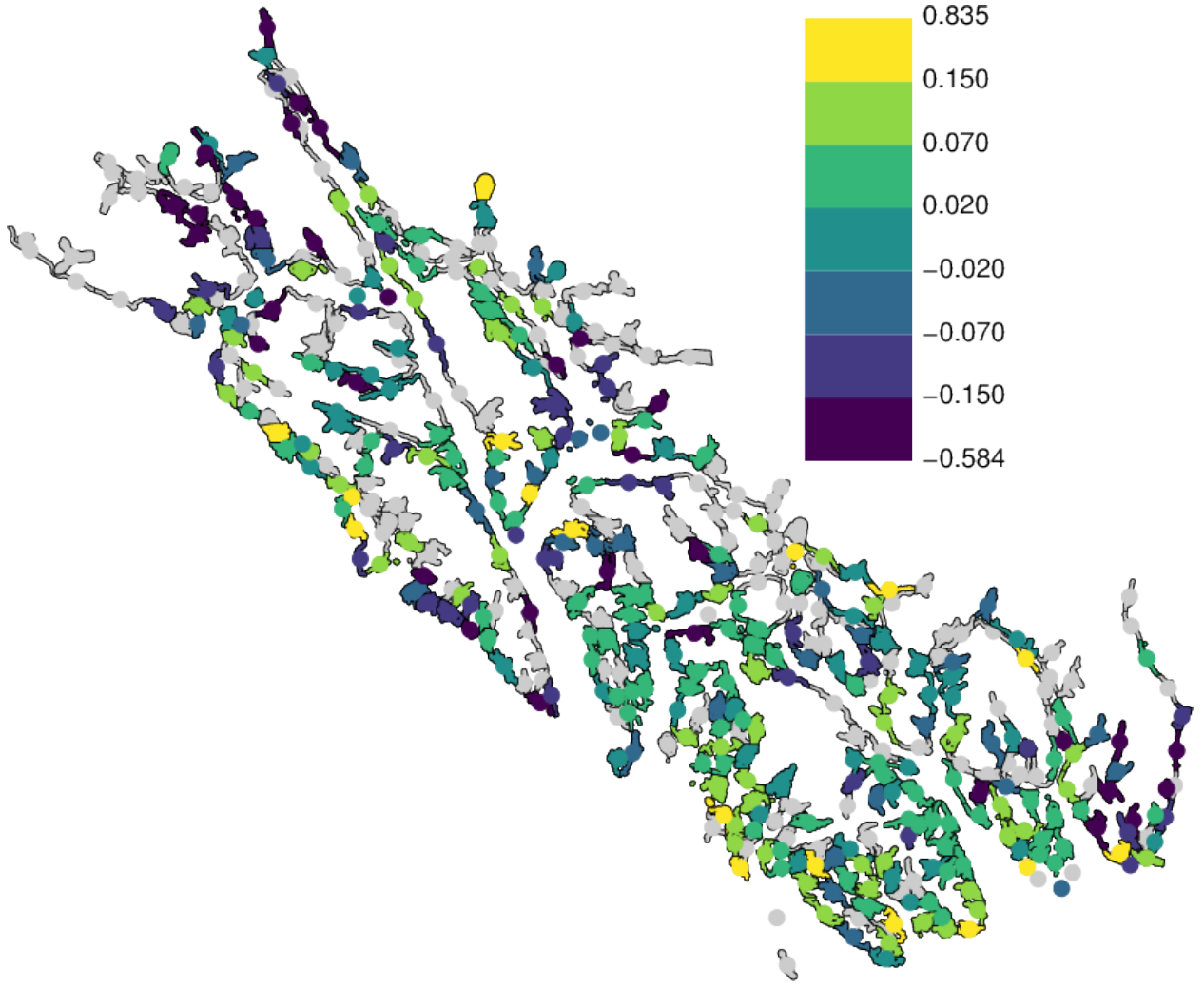


Figure 2: Map of the estimated trends (used as our raw data), where polygons are colored by their trend values. The light grey polygons have missing data. Because some polygons were small and it was difficult to see colors in them, all polygons were also overwritten by a circle of the same color. The trend values were categorized by colors, with increasing trends in yellows and greens, and decreasing trends in blues and violets, with the cutoff values given by the color ramp.

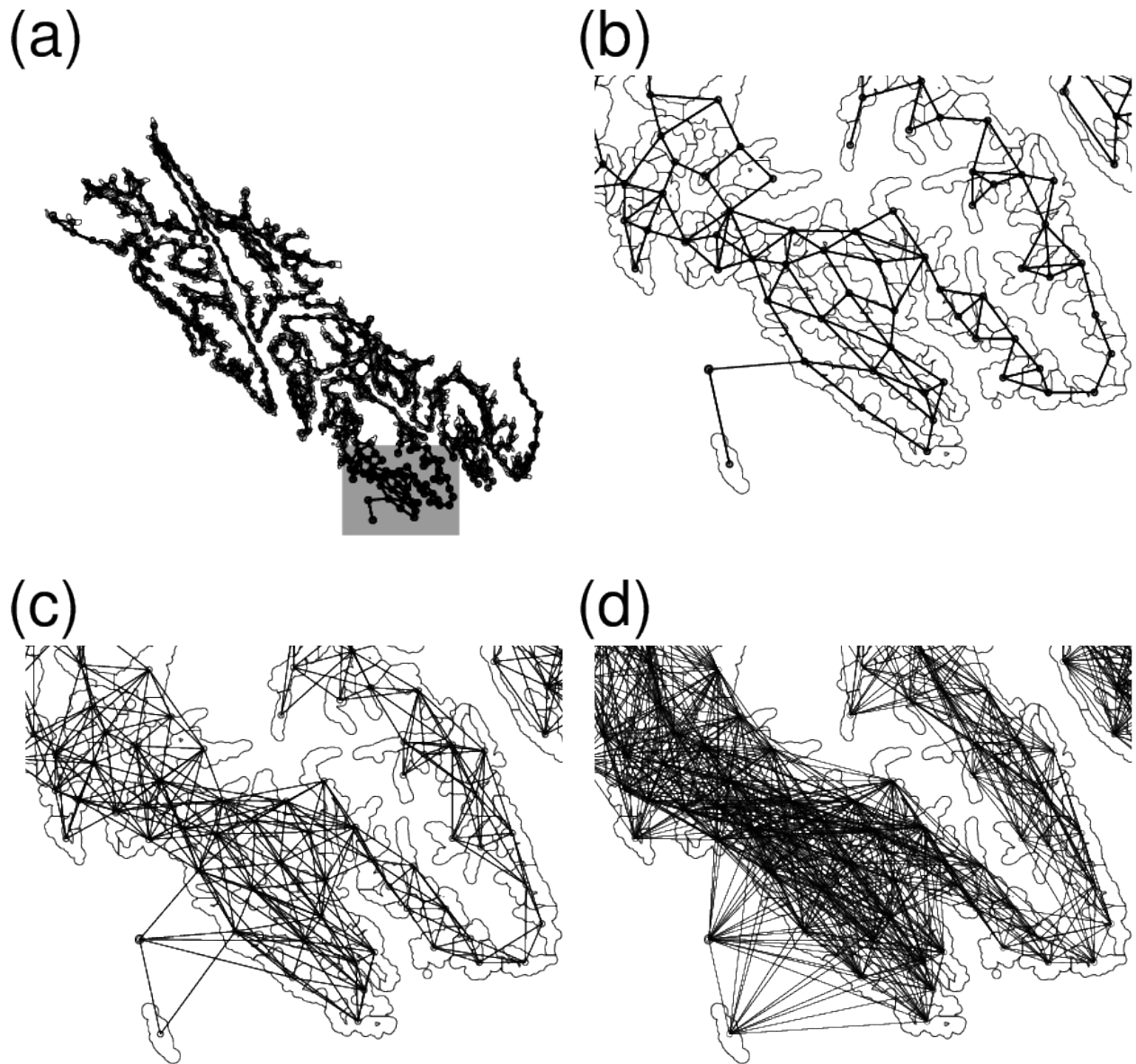


Figure 3: First, second, and fourth-order neighbor definitions for the survey polygons. (a) First-order neighbors for all polygons. The grey rectangle is the area for a closer view in the following subfigures: (b) first-order neighbors; (c) second-order neighbors; and (d) fourth-order neighbors.

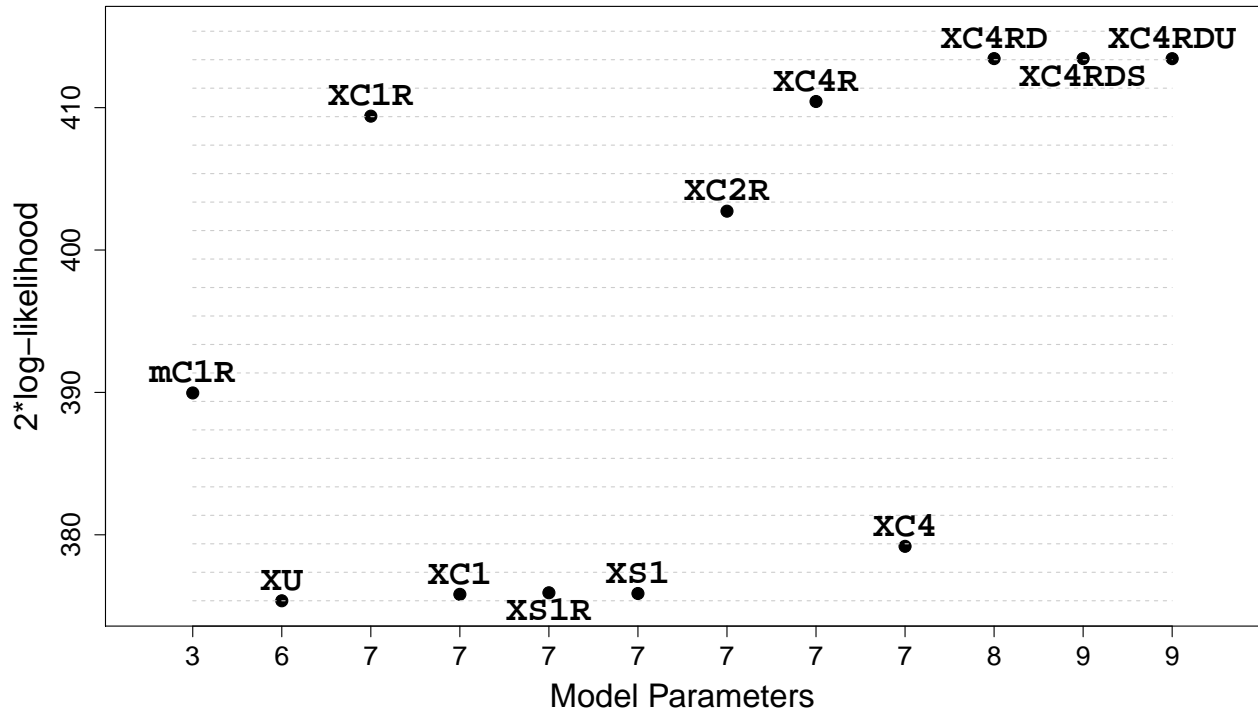


Figure 4: Two times the log-likelihood for the optimized (maximized) fit for the models given in Table 2. Model mU had a much lower value (350.2) and is not shown. Starting with model XU, the dashed grey lines show increments of 2, which helps evaluate the relative importance of models by either an AIC or a likelihood-ratio test criteria.

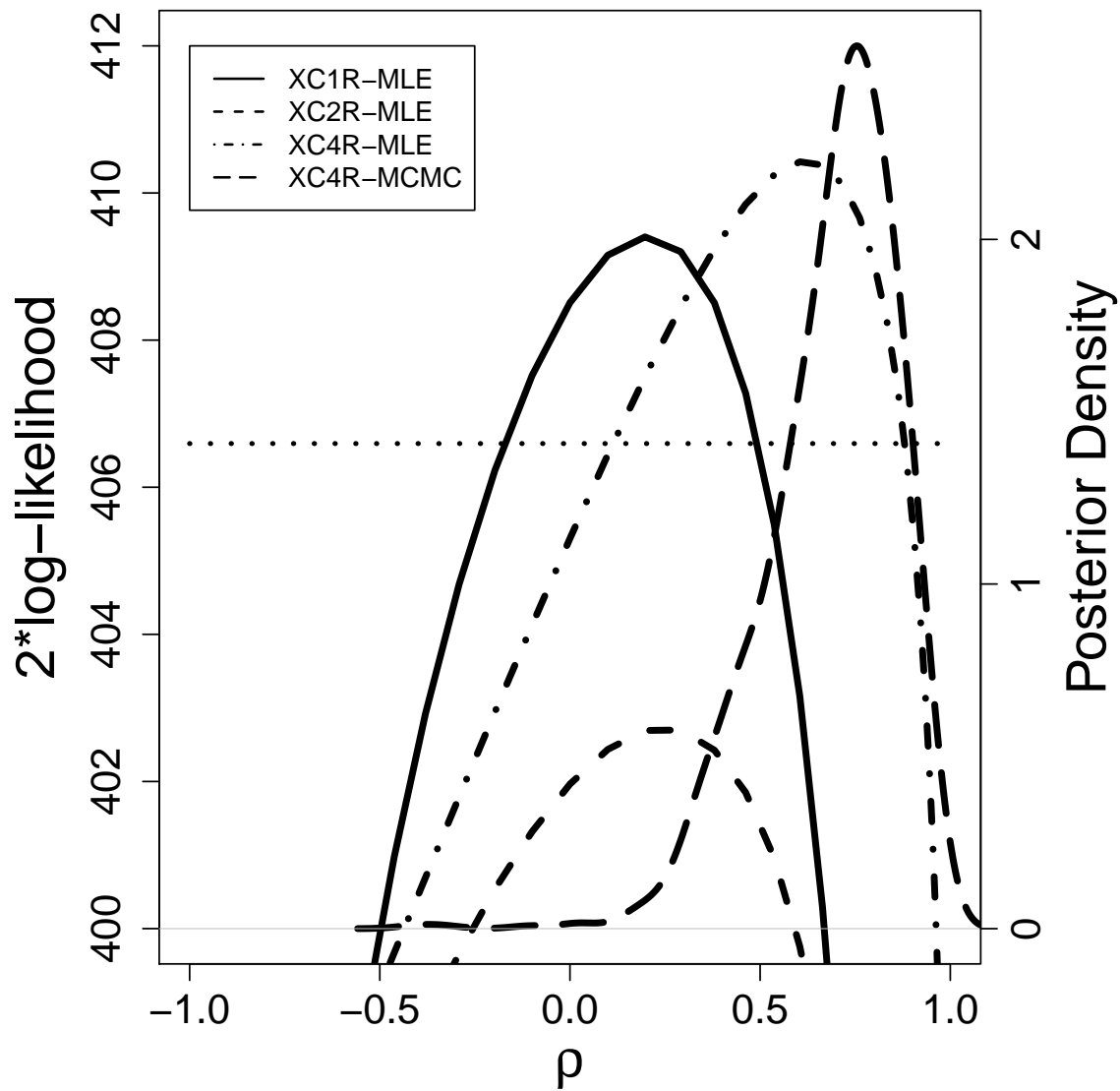


Figure 5: The different lines show $2 \cdot \log\text{-likelihood}$ profiles of ρ for three different models, listed in the legend. If the model is followed by -MLE, then the maximum of the profile provides the maximum likelihood estimate, and the $2 \cdot \log\text{-likelihood}$ is given by the left y-axis, while if it is followed by MCMC, then it is the posterior distribution from a Bayesian model with a uniform prior on ρ , and the density is given by the right y-axis. The horizontal dotted line is the maximum value for XC4R minus 3.841, the 0.05 α -level value of a χ -squared distribution on one degree of freedom.

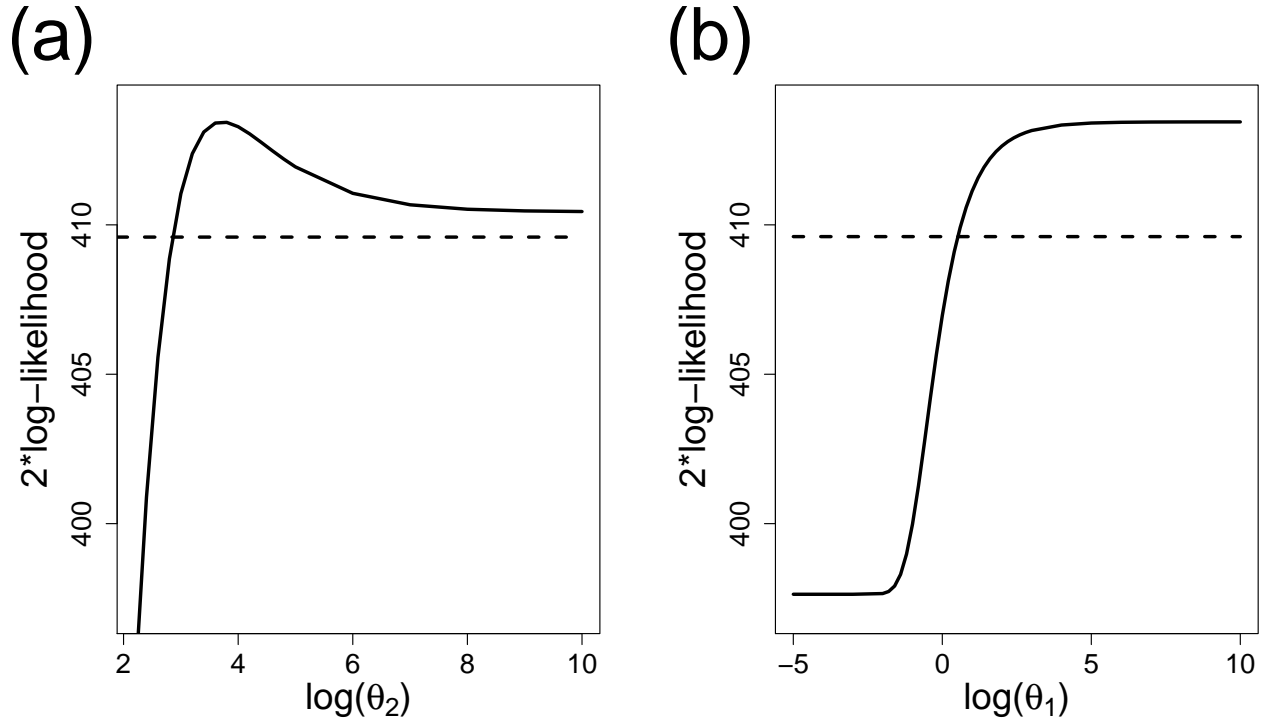


Figure 6: A) The solid line is the 2*Log-likelihood profile of θ_2 for model XC4RD. B) The solid line is the 2*Log-likelihood profile of θ_1 for model XC4RDS. For each figure, the horizontal dashed line is the maximum value for the model minus 3.841, the 0.05 α -level value of a χ -squared distribution on one degree of freedom.

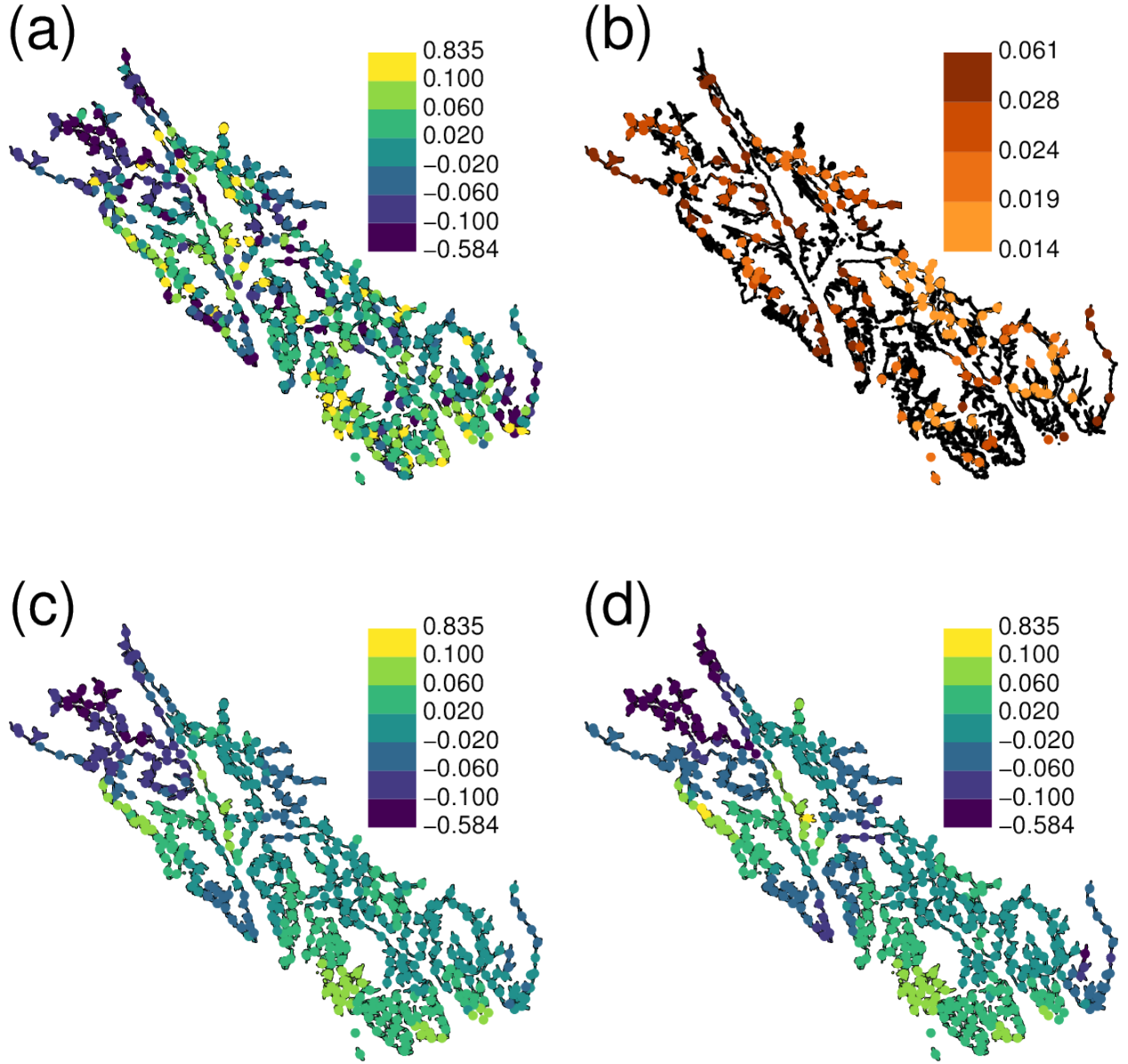


Figure 7: Predictions and smoothing for the harbor-seal stock-trend data. (a) Predictions, using universal kriging from the XC4R model, at unsampled locations have been added to the raw observed data from sampled locations. (b) Prediction standard errors for unsampled locations using universal kriging from XC4R. (c) Smoothing over all locations using conditional expectation based on the XC4R model. (d) Smoothing over all locations by using posterior predictions (mean of posterior distributions) using the XI4RU model in a Bayesian hierarchical model.

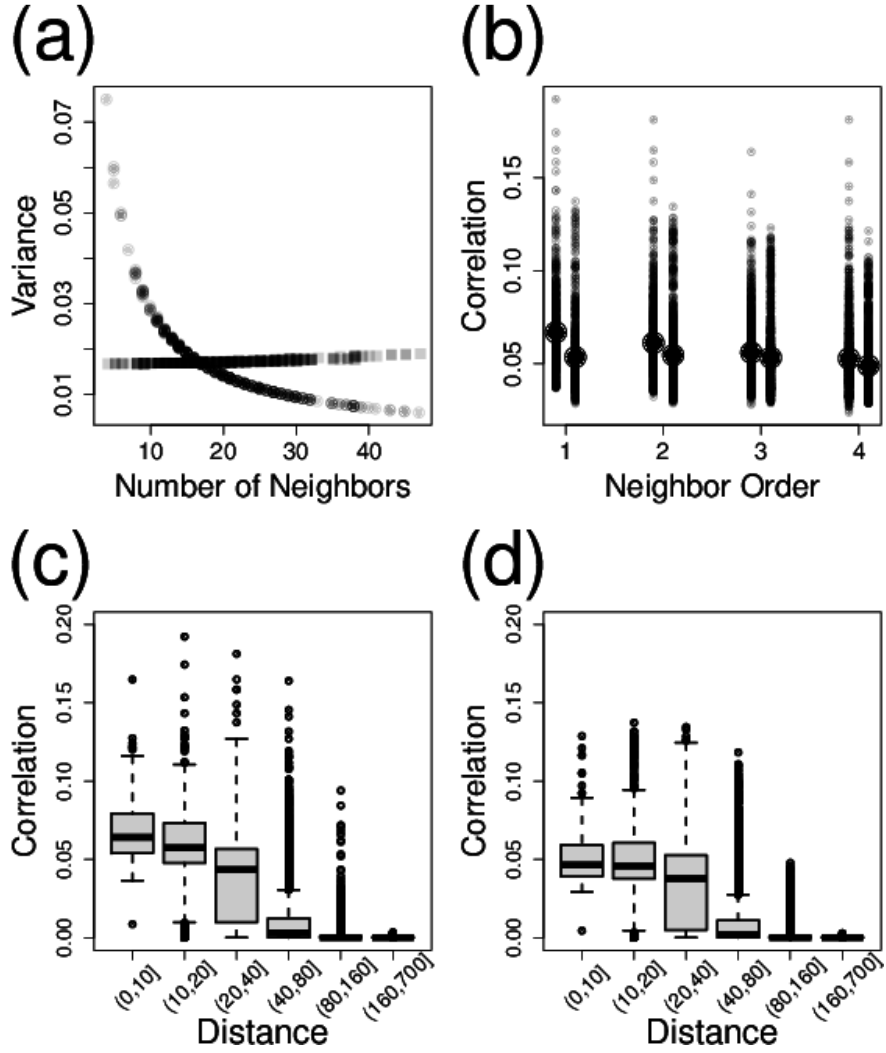


Figure 8: Nonstationarity illustrated for XC4 model, and the same model using row-standardization, XC4R. A) Marginal variances of the multivariate covariance matrix (diagonal elements of Σ) as a function of the numbers of neighbors, where circles indicate XC4R and squares indicate XC4. Each symbol is partially transparent. B) All pairwise correlations as a function of the neighborhood order between sites. On the left of each neighbor order is XC4R, and on the right is XC4. The larger circle is the average value. C) and D) Boxplots of pairwise correlation as a function of distance between polygon centroids, binned into classes, for models XC4R and XC4, respectively.

1 APPENDIX A: Misconceptions and Errors in the Literature

The fact that CAR and SAR models are developed for the precision matrix, in contrast to geostatistical models being developed for the covariance matrix, has caused some confusion in the ecological literature. For example, in comparing geostatistical models to SAR models, Beguería and Pueyo (2009) stated “Semivariogram models account for spatial autocorrelation *at all possible distance lags*, and thus they do not require *a priori* specification of the window size and the covariance structure,” (emphasis by the original authors). CAR and SAR models also account for spatial autocorrelation at all possible lags, as seen in Fig. 8c,d. In a temporal analogy, the autoregressive AR1 time series models also account for autocorrelation at all possible lags, where the conditional specification $Z_{i+1} = \phi Z_i + \nu_i$, with ν_i an independent random shock and $|\phi| < 1$, implies that $\text{corr}(Z_i, Z_{i+t}) = \phi^t$ for all t . In fact, if we restrict $0 < \phi < 1$, then this can be reparameterized as $\text{corr}(Z_i, Z_{i+t}) = \exp(-t(-\log(\phi)))$, which is an exponential geostatistical model with range parameter $-\log(\phi)$. While there are interesting results in Beguería and Pueyo (2009), a restriction on the range of autocorrelation is not a reason that CAR/SAR models might perform poorly against a geostatistical model. The important concept is that the autoregressive specification is local in the precision matrix and not in the covariance matrix.

CAR models are often incorrectly characterized. For example, Keitt et al. (2002) characterized CAR models as: $\mathbf{Y} = \mathbf{X}\boldsymbol{\beta} + \rho\mathbf{C}(\mathbf{Y} - \mathbf{X}\boldsymbol{\beta}) + \boldsymbol{\varepsilon}$, with a stated covariance matrix of $\sigma^2(\mathbf{I} - \rho\mathbf{C})^{-1}$, where \mathbf{C} is symmetric. Their actual implementation may have been correct, and there are excellent and important results in Keitt et al. (2002); however, the construction they used leads to a SAR covariance matrix of $\sigma^2(\mathbf{I} - \rho\mathbf{C})^{-1}(\mathbf{I} - \rho\mathbf{C})^{-1}$ if $\text{var}(\boldsymbol{\varepsilon}) = \sigma^2\mathbf{I}$ and \mathbf{C} is symmetric. Even to characterize a CAR model as $\sigma^2(\mathbf{I} - \rho\mathbf{C})^{-1}$ with symmetric \mathbf{C} is overly restrictive, as we have demonstrated that an asymmetric \mathbf{C} with the proper \mathbf{M} will still satisfy

Eq. 8, or alternatively that $\Sigma^{-1} = (\mathbf{M}^{-1} - \mathbf{C})/\sigma^2$, where \mathbf{C} is symmetric but \mathbf{M}^{-1} is not necessarily constant on the diagonals. In fact, constraining a CAR model to $\sigma^2(\mathbf{I} - \rho\mathbf{C})^{-1}$ does not allow for row-standardized models. These mistakes are perpetuated in Dormann et al. (2007), and we have seen similar errors in describing CAR models as SAR models in other literature, presentations, and help sites on the internet.

Dormann et al. (2007) also claimed that any SAR model is a CAR model, which agrees with the literature (e.g., Cressie, 1993, p. 409), but then they show an incorrect proof (it is also incorrect in Haining (1990, p. 89), and likely beginning there), because they do not consider that \mathbf{C} for a CAR model must have zeros along the diagonal. In fact, we demonstrate in Appendix B that, despite statistical and ecological literature to the contrary, CAR models and SAR models can be written equivalently, and we provide details.

2 APPENDIX B: Equivalence of CAR and SAR Models

In what follows, for matrices denoted with bold capital letters, let their i th column and j row be denoted with small case letters with subscripts i, j ; for example, the i, j th element of \mathbf{C} is c_{ij} .

Assume \mathbf{M} and $\mathbf{\Lambda}$ are diagonal matrices. To establish when CAR models can be written as SAR, and vice versa, we need the following equality,

$$(\mathbf{I} - \mathbf{C})^{-1}\mathbf{M} = (\mathbf{I} - \mathbf{B})^{-1}\mathbf{\Lambda}(\mathbf{I} - \mathbf{B}')^{-1}, \quad (\text{B.1})$$

satisfying, for the CAR covariance matrix on the left-hand side,

1) $(\mathbf{I} - \mathbf{C})^{-1}$ exists,

2) $c_{ii} = 0, \forall i$, and

3) $c_{ij}/m_{ii} = c_{ji}/m_{jj}, \forall i, j$;

and for the SAR covariance matrix on the right-hand side,

4) $(\mathbf{I} - \mathbf{B})^{-1}$ exists, and

5) $b_{ii} = 0, \forall i$.

Notice that we write the SAR covariance matrix as $(\mathbf{I} - \mathbf{B})^{-1}\mathbf{\Lambda}(\mathbf{I} - \mathbf{B}')^{-1}$, where $\mathbf{\Lambda}$ is a diagonal matrix, in Eq. B.1, following Cressie (1993, p. 409), which is a little more general than the SAR covariance matrix given in Eq. 2. Ultimately, this demonstration relies on establishing that any zero-mean Gaussian distribution on a finite set of points, $\mathbf{Z} \sim N(\mathbf{0}, \mathbf{\Sigma})$, can be written as either the left-hand side, or the right-hand side of Eq. B.1. Note, we make use of the following results. If \mathbf{D} is diagonal, and \mathbf{Q} has zero on the diagonals, then both \mathbf{DQ} and \mathbf{QD} have zeros on the diagonal. If $\mathbf{A} = \mathbf{BC}$, and \mathbf{A} and \mathbf{C} have inverses, then \mathbf{B} has an inverse.

First consider obtaining the left-hand side of Eq. B.1; this result is also given by Cressie (1993, p. 434). Write $\Sigma^{-1} = \mathbf{D} - \mathbf{Q}$, where \mathbf{D} is diagonal and \mathbf{Q} has zeros on the diagonal. Then factor out \mathbf{D} so that $\Sigma^{-1} = \mathbf{D}(\mathbf{I} - \mathbf{D}^{-1}\mathbf{Q})$, and now let $\mathbf{M} = \mathbf{D}^{-1}$ and $\mathbf{C} = \mathbf{D}^{-1}\mathbf{Q}$, then $(\mathbf{I} - \mathbf{C})^{-1}$ exists because Σ^{-1} and \mathbf{D}^{-1} exist, \mathbf{C} will have zeros on the diagonals, and condition 3) is satisfied by construction (because it is the requirement for symmetry). Thus, Σ^{-1} can be expressed as $\mathbf{M}^{-1}(\mathbf{I} - \mathbf{C})$ and $\Sigma = (\mathbf{I} - \mathbf{C})^{-1}\mathbf{M}$ satisfying conditions 1) to 3).

Next, consider the right-hand side of Eq. B.1. Write $\Sigma^{-1} = \mathbf{L}\mathbf{L}'$, and suppose that \mathbf{L} has an inverse. Note that \mathbf{L} is *not* unique. A Cholesky decomposition satisfies this, where \mathbf{L} is lower triangular, or a singular value decomposition could be used, where $\Sigma = \mathbf{V}\mathbf{E}\mathbf{V}'$ with \mathbf{V} containing orthonormal eigenvectors and \mathbf{E} containing eigenvalues. Then $\mathbf{L} = \mathbf{V}\mathbf{E}^{-1/2}\mathbf{V}'$. In any case, let $\mathbf{L}\mathbf{L}' = (\mathbf{G} - \mathbf{P})(\mathbf{G}' - \mathbf{P}')$, where \mathbf{G} is diagonal and \mathbf{P} has zero diagonals. Then factor out \mathbf{G} to obtain $\mathbf{L}\mathbf{L}' = (\mathbf{I} - \mathbf{P}\mathbf{G}^{-1})\mathbf{G}\mathbf{G}(\mathbf{I} - \mathbf{G}^{-1}\mathbf{P}')$, and now let $\mathbf{A}^{-1} = \mathbf{G}\mathbf{G}$ and $\mathbf{B}' = \mathbf{P}\mathbf{G}^{-1}$. Notice that $(\mathbf{P}\mathbf{G}^{-1})' = \mathbf{G}^{-1}\mathbf{P}'$ because \mathbf{G}^{-1} is diagonal. Thus, Σ^{-1} can be expressed as $(\mathbf{I} - \mathbf{B}')\mathbf{A}^{-1}(\mathbf{I} - \mathbf{B})$ and $\Sigma = (\mathbf{I} - \mathbf{B})^{-1}\mathbf{A}(\mathbf{I} - \mathbf{B}')^{-1}$. Moreover, $(\mathbf{I} - \mathbf{B})^{-1}$ exists because \mathbf{L}^{-1} and \mathbf{G}^{-1} exist and \mathbf{B} will have zeros on the diagonals, satisfying conditions 4) and 5). Note that in order to write it as $(\mathbf{I} - \mathbf{B})^{-1}(\mathbf{I} - \mathbf{B}')^{-1}$, we would need to find \mathbf{L} with ones on the diagonal so that $\mathbf{G} = \mathbf{I}$.

Hence, we have demonstrated that any zero-mean Gaussian distribution on a finite set of points, $\mathbf{Z} \sim \mathcal{N}(\mathbf{0}, \Sigma)$ can be written as either the left-hand side, or the right-hand side of Eq. B.1, with the important difference that a CAR model is uniquely determined from Σ but a SAR model is not so uniquely determined. That a CAR is unique is easy to see from the algebra used to derive it. To see more fully why a SAR model is not uniquely determined, let \mathbf{A} be a matrix with orthonormal columns, and notice that $\Sigma^{-1} = \mathbf{L}\mathbf{L}' = \mathbf{L}(\mathbf{A}'\mathbf{A})\mathbf{L}' = (\mathbf{L}\mathbf{A}')(\mathbf{A}\mathbf{L}') = \mathbf{L}_*\mathbf{L}_*'$. A SAR model can be developed as readily for \mathbf{L}_* as for \mathbf{L} . In fact, if we think of \mathbf{A} as coordinate vectors, any rotation of the matrix \mathbf{A} will create yet another SAR model, so there are an infinite

1037 number of them.

1038 With this appendix, we also wish to correct an error that has been perpetuating in the
1039 literature, beginning with Haining (1990, p. 89), and we also found it in Schabenberger and
1040 Gotway (2005) and Dormann et al. (2007). The authors assume in Eq. B.1 that $\mathbf{M} = \mathbf{I}$ and
1041 $\mathbf{A} = \mathbf{I}$, so that \mathbf{C} is symmetric. That implies that $(\mathbf{I} - \mathbf{C})^{-1} = [(\mathbf{I} - \mathbf{B})(\mathbf{I} - \mathbf{B}')]^{-1}$
1042 $= (\mathbf{I} - \mathbf{B} - \mathbf{B}' + \mathbf{B}\mathbf{B}')^{-1}$, and the claim is that this shows how any SAR can be easily made into a
1043 CAR by setting $\mathbf{C} = \mathbf{B} + \mathbf{B}' - \mathbf{B}\mathbf{B}'$. However, while $\mathbf{C} = \mathbf{B} + \mathbf{B}' - \mathbf{B}\mathbf{B}'$ is sufficient for equality, it
1044 is not necessary, and it lacks a critical component; that $\mathbf{B} + \mathbf{B}' - \mathbf{B}\mathbf{B}'$ must have zeros on the
1045 diagonal for \mathbf{C} to be a CAR model. The proper way to proceed was outlined above, by letting
1046 $\mathbf{C} = \mathbf{D}^{-1}\mathbf{Q}$ in the equality

$$(\mathbf{I} - \mathbf{D}^{-1}\mathbf{Q})^{-1}\mathbf{D}^{-1} = (\mathbf{I} - \mathbf{B} - \mathbf{B}' + \mathbf{B}\mathbf{B}')^{-1},$$

1047 where the left-hand side is uniquely determined from the right-hand side, and \mathbf{C} satisfies the
1048 requirement for a CAR model. As we demonstrated in the previous paragraph, it is not possible
1049 to go uniquely from the left-hand side to the right-hand side without additional constraints.

3 APPENDIX C: Maximum Likelihood Estimation for

CAR/SAR Models with Missing Data

We begin by finding analytical solutions when we can, and then substituting them into the likelihood to reduce the number of parameters as much as possible for the full covariance matrix.

Assume a linear model,

$$\mathbf{y} = \mathbf{X}\boldsymbol{\beta} + \boldsymbol{\varepsilon},$$

where \mathbf{y} is a vector of response variables, \mathbf{X} is a design matrix of full rank, $\boldsymbol{\beta}$ is a vector of parameters, and the zero-mean random errors have a multivariate normal distribution, $\boldsymbol{\varepsilon} \sim N(\mathbf{0}, \boldsymbol{\Sigma})$, where $\boldsymbol{\Sigma}$ is a patterned covariance matrix; i.e., it has non-zero off-diagonal elements.

Suppose that $\boldsymbol{\Sigma}$ has parameters $\{\theta, \boldsymbol{\rho}\}$ and can be written as $\boldsymbol{\Sigma} = \theta \mathbf{V}_{\boldsymbol{\rho}}$, where θ is an overall variance parameter and $\boldsymbol{\rho}$ are parameters that structure $\mathbf{V}_{\boldsymbol{\rho}}$ as a non-diagonal matrix, and we show the dependency as a subscript. Note that $\boldsymbol{\Sigma}^{-1} = \mathbf{V}_{\boldsymbol{\rho}}^{-1}/\theta$. Recall that the maximum likelihood estimate of $\boldsymbol{\beta}$ for any $\{\theta, \boldsymbol{\rho}\}$ is $\hat{\boldsymbol{\beta}} = (\mathbf{X}'\mathbf{V}_{\boldsymbol{\rho}}^{-1}\mathbf{X})^{-1}\mathbf{X}'\mathbf{V}_{\boldsymbol{\rho}}^{-1}\mathbf{y}$. By substituting $\hat{\boldsymbol{\beta}}$ into the normal likelihood equations, -2 times the loglikelihood for a normal distribution is

$$\mathcal{L}(\theta, \boldsymbol{\rho}|\mathbf{y}) = (\mathbf{y} - \mathbf{X}\hat{\boldsymbol{\beta}})' \boldsymbol{\Sigma}^{-1} (\mathbf{y} - \mathbf{X}\hat{\boldsymbol{\beta}}) + \log(|\boldsymbol{\Sigma}|) + n\log(2\pi),$$

where n is the length of \mathbf{y} , but this can be written as,

$$\mathcal{L}(\theta, \boldsymbol{\rho}|\mathbf{y}) = \mathbf{r}_{\boldsymbol{\rho}}' \mathbf{V}_{\boldsymbol{\rho}}^{-1} \mathbf{r}_{\boldsymbol{\rho}} / \theta + n\log(\theta) + \log(|\mathbf{V}|) + n\log(2\pi) \quad (\text{C.1})$$

1064 where $\mathbf{r}_\rho = (\mathbf{y} - \mathbf{X}\hat{\boldsymbol{\beta}})$ (notice that $\hat{\boldsymbol{\beta}}$ is a function of $\boldsymbol{\rho}$, so we show that dependency for \mathbf{r} as well).

1065 Conditioning on $\boldsymbol{\rho}$ yields

$$\mathcal{L}(\theta|\boldsymbol{\rho}, \mathbf{y}) = \mathbf{r}'_\rho \mathbf{V}_\rho^{-1} \mathbf{r}_\rho / \theta + n \log(\theta) + \text{terms not containing } \theta$$

1066 and minimizing for θ involves setting

$$\frac{\partial \mathcal{L}(\theta|\boldsymbol{\rho}, \mathbf{y})}{\partial \theta} = -\mathbf{r}'_\rho \mathbf{V}_\rho^{-1} \mathbf{r}_\rho / \theta^2 + n / \theta$$

1067 equal to zero, yielding the maximum likelihood estimate

$$\hat{\theta} = \mathbf{r}'_\rho \mathbf{V}_\rho^{-1} \mathbf{r}_\rho / n. \quad (\text{C.2})$$

1068 Substituting Eq. C.2 back into Eq. C.1 yields the -2*loglikelihood as a function of $\boldsymbol{\rho}$ only,

$$\mathcal{L}(\boldsymbol{\rho}|\mathbf{y}) = n \log(\mathbf{r}'_\rho \mathbf{V}_\rho^{-1} \mathbf{r}_\rho) + \log(|\mathbf{V}_\rho|) + n(\log(2\pi) + 1 - \log(n)). \quad (\text{C.3})$$

1069 Equation Eq. C.3 can be minimized numerically to yield the MLE $\hat{\boldsymbol{\rho}}$, and then $\hat{\theta} = \mathbf{r}'_{\hat{\boldsymbol{\rho}}} \mathbf{V}_{\hat{\boldsymbol{\rho}}}^{-1} \mathbf{r}_{\hat{\boldsymbol{\rho}}} / n$,

1070 and $\hat{\boldsymbol{\beta}} = (\mathbf{X}' \mathbf{V}_{\hat{\boldsymbol{\rho}}}^{-1} \mathbf{X})^{-1} \mathbf{X}' \mathbf{V}_{\hat{\boldsymbol{\rho}}}^{-1} \mathbf{y}$.

1071 We developed the inverse covariance matrix $\boldsymbol{\Sigma}_A^{-1} = \text{diag}(\mathbf{W}\mathbf{1}) - \rho \mathbf{W}$, and here we use $\boldsymbol{\Sigma}_A$

1072 to denote it is for *all* locations, those with observed data as well as those without. Without

1073 missing data, Eq. C.3 can be evaluated quickly by factoring out an overall variance parameter

1074 from $\boldsymbol{\Sigma}_A^{-1}$ and using sparse matrix methods to quickly and efficiently evaluate $|\mathbf{V}_\rho|$ by recalling

1075 that $|\mathbf{V}_\rho| = 1/|\mathbf{V}_\rho^{-1}|$. However, when there are missing data, there is no guarantee that \mathbf{V}_ρ will

1076 be sparse. The obvious and direct approach is to first obtain $\boldsymbol{\Sigma}_A = (\boldsymbol{\Sigma}_A^{-1})^{-1}$, and then obtain

1077 $\mathbf{V}_\rho = \mathbf{\Sigma}[\mathbf{i}, \mathbf{i}]$, where \mathbf{i} is a vector of indicators that subsets the rows and columns of $\mathbf{\Sigma}$ to only
 1078 those for sampled locations. Then, a third step is a second inverse to find \mathbf{V}_ρ^{-1} . However, this is
 1079 computationally expensive. A faster way uses results from partitioned matrices and Schur
 1080 complements. In general, let the square matrix $\mathbf{\Sigma}$ with dimensions $(m+n) \times (m+n)$ be
 1081 partitioned into block submatrices,

$$\mathbf{\Sigma}_{(m+n) \times (m+n)} = \begin{bmatrix} \mathbf{A}_{m \times m} & \mathbf{B}_{m \times n} \\ \mathbf{C}_{n \times m} & \mathbf{D}_{n \times n} \end{bmatrix}$$

1082 with dimensions given below each matrix. Assume \mathbf{A} and \mathbf{D} are nonsingular. Then define the
 1083 matrix function $\mathbf{S}(\mathbf{\Sigma}, \mathbf{A}) = \mathbf{D} - \mathbf{CA}^{-1}\mathbf{B}$ as the Schur complement of $\mathbf{\Sigma}$ with respect to \mathbf{A} .
 1084 Likewise, there is a Schur complement with respect to \mathbf{D} by reversing the roles of \mathbf{A} and \mathbf{D} .
 1085 Using Schur complements, it is well-known (e.g, Harville, 1997, p. 97) that an inverse for a
 1086 partitioned matrix $\mathbf{\Sigma}$ is,

$$\mathbf{\Sigma}^{-1} = \begin{bmatrix} \mathbf{A}^{-1} + \mathbf{A}^{-1}\mathbf{BS}(\mathbf{\Sigma}, \mathbf{A})^{-1}\mathbf{CA}^{-1} & -\mathbf{A}^{-1}\mathbf{BS}(\mathbf{\Sigma}, \mathbf{A})^{-1} \\ -\mathbf{S}(\mathbf{\Sigma}, \mathbf{A})^{-1}\mathbf{CA}^{-1} & \mathbf{S}(\mathbf{\Sigma}, \mathbf{A})^{-1} \end{bmatrix}$$

1087 Then, note that $\mathbf{A}^{-1} = \mathbf{S}(\mathbf{\Sigma}^{-1}, \mathbf{S}(\mathbf{\Sigma}, \mathbf{A})^{-1})$; that is, if we already have $\mathbf{\Sigma}^{-1}$, then \mathbf{A}^{-1} is the
 1088 Schur complement of $\mathbf{\Sigma}^{-1}$ with respect to the rows and columns that correspond to \mathbf{D} .
 1089 Additionally, the largest matrix that we have to invert is $[\mathbf{S}(\mathbf{\Sigma}, \mathbf{A})^{-1}]^{-1}$, which is $n \times n$, which has
 1090 dimension less than $\mathbf{\Sigma}$, and only one inverse is required. So, if we let \mathbf{A} correspond to the rows
 1091 and columns of the observed locations, and \mathbf{D} correspond to the rows and columns of the missing
 1092 data, then this provides a quick and efficient way to obtain \mathbf{V}_ρ^{-1} from $\mathbf{\Sigma}_A^{-1}$, and the largest inverse
 1093 required is $n \times n$, the number of missing data.

4 APPENDIX D: Prediction and Smoothing

Here, we provide the formulas used in creating Fig. 7. For universal kriging, the formulas can be found in Cressie and Wikle (2011, p. 148),

$$\hat{y}_i = \mathbf{x}_i' \hat{\boldsymbol{\beta}} + \mathbf{c}_i \boldsymbol{\Sigma}_{-i}^{-1} (\mathbf{y}_{-i} - \mathbf{X} \hat{\boldsymbol{\beta}})$$

where \hat{y}_i is the prediction for the i th node, \mathbf{x}_i is a vector containing the covariate values for the i th node, \mathbf{X} is the design matrix for the covariates (fixed effects), \mathbf{c}_i is a vector containing the fitted covariance between the i th site and all *other* sites with observed data, $\boldsymbol{\Sigma}$ is the fitted covariance matrix among all observed data, \mathbf{y} is a vector of observed values for the response variable, and $\hat{\boldsymbol{\beta}} = \mathbf{X}'(\mathbf{X}'\boldsymbol{\Sigma}^{-1}\mathbf{X})^{-1}\mathbf{X}'\boldsymbol{\Sigma}^{-1}\mathbf{y}$ is the generalized least squares estimate of $\boldsymbol{\beta}$. The covariance values contained in \mathbf{c}_i and $\boldsymbol{\Sigma}$ were obtained using maximum likelihood estimate for the parameters as detailed in Appendix C. We include the $-i$ subscript on $\boldsymbol{\Sigma}_{-i}^{-1}$ and \mathbf{y}_{-i} to indicate that, when smoothing, we predict at the i th node by removing that datum from \mathbf{y} , and by removing its corresponding rows and columns in $\boldsymbol{\Sigma}$. If the value is missing, then prediction proceeds using all observed values. Hence, Fig. 7a contains the observed values plus the predicted values at nodes with missing values, while Fig. 7c contains predicted values at all nodes, where any observed value at a node was removed and predicted with the rest of the observed values. The prediction standard errors are given by,

$$\widehat{\text{se}}(\hat{y}_i) = \sqrt{\mathbf{c}_i' \boldsymbol{\Sigma}_{-i}^{-1} \mathbf{c}_i + \mathbf{d}_i' (\mathbf{X}_{-i}' \boldsymbol{\Sigma}_{-i}^{-1} \mathbf{X}_{-i})^{-1} \mathbf{d}_i}$$

where $\mathbf{d}_i = \mathbf{x}_i' - \mathbf{X}_{-i}' \boldsymbol{\Sigma}_{-i}^{-1} \mathbf{c}_i$.

For the IAR model smoothing in Fig. 7d, we used the WinBUGS (Lunn et al., 2000)

1112 software, final version 1.4.3. The model code is very compact and given below:

```
model
{
  for(i in 1:N) {
    trend[i] ~ dnorm(mu[i],prec)
    mu[i] <- beta0 + beta[stockid[i]] + b[i]
  }
  b[1:N] ~ car.normal(adj[], weights[], num[], tau)
  beta0 ~ dnorm(0,.001)
  beta[1] ~ dnorm(0,.001)
  beta[2] ~ dnorm(0,.001)
  beta[3] ~ dnorm(0,.001)
  beta[4] <- 0
  beta[5] ~ dnorm(0,.001)
  prec ~ dgamma(0.001,0.001)
  sigmaEps <- sqrt(1/prec)
  tau ~ dgamma(0.5, 0.0005)
  sigmaZ <- sqrt(1 / tau)
}
```

1113 The means of the MCMC samples from the posterior distributions of $\mu[i]$ were used for the

1114 IAR smoothing for the i th location in Fig. 7d.